NTIA Technical Memorandum TM-06-439

Resolving Interference from an Airport Surveillance Radar to a Weather Radar

Frank H. Sanders
J. Randy Hoffman
Yeh Lo

technical memorandum

U.S. DEPARTMENT OF COMMERCE • National Telecommunications and Information Administration

NTIA Technical Memorandum TM-06-439

Resolving Interference from an Airport Surveillance Radar to a Weather Radar

Frank H. Sanders
J. Randy Hoffman
Yeh Lo

U.S. DEPARTMENT OF COMMERCE
Carlos M. Gutierrez, Secretary

John M. R. Kneuer, Acting Assistant Secretary
for Communications and Information

April 2006

ACKNOWLEDGEMENTS

The work described in this report was performed under an other-agency agreement between NTIA and the National Weather Service (NWS). The results reported here were obtained as a result of close coordination and cooperation between many personnel of NWS, NTIA, and the Federal Aviation Administration (FAA). The work was performed at a field location of an airport surveillance radar and a weather radar at Ft. Smith, AR, during the dates of January 24-26, 2006. During those tests, the assistance of the following NWS personnel was essential to the successful outcome of the work: Mr. Russell Cook, Mr. T. Lynn Allmon, Mr. Glenn Secrest, and Ms. Felicia Willard. FAA personnel who made important contributions included Mr. Timothy Pawlowitz, Mr. Dan Hicok, and Mr. Allen Cloud. Ms. Iris Tobias of NTIA provided important on-site support during the measurements, and also drove the RSMS-4 measurement truck to and from the site.

DISCLAIMER

Certain commercial equipment and materials are identified in this report to specify adequately the technical aspects of the reported results. In no case does such identification imply recommendations or endorsement by the National Telecommunications and Information Administration, nor does it imply that the material or equipment identified is the best available for this purpose.

CONTENTS

Page

FIGURES

Page

TABLES

ABBREVIATIONS/ACRONYMS

ASR airport surveillance radar

EMI electromagnetic interference mitigation filter

FAA Federal Aviation Administration

I interference power level

IF intermediate frequency stage of a receiver

I/N interference to noise ratio in receiver IF stage

ITS Institute for Telecommunication Sciences

LNA low noise amplifier

N noise power level

NTIA National Telecommunications and Information Administration

NWS National Weather Service

PDL passive diode limiter

RSEC Radar Spectrum Engineering Criteria

RSMS-4 Radio Spectrum Measurement System, fourth generation

RBW resolution bandwidth

RSL received signal level

OOB out-of-band emission type

YIG yttrium iron garnet filter technology

RESOLVING INTERFERENCE FROM AN AIRPORT SURVEILLANCE RADAR TO A WEATHER RADAR

Frank H. Sanders, J. Randall Hoffman, and Yeh Lo[1]

In response to interference from an S-band (2700-2900 MHz) airport surveillance radar (ASR) to a meteorological (weather) radar in the same band, measurements were performed at the field location of the two radars to determine the interference mechanism and any possible mitigation options. Measurements included emission spectra of the ASR and observations of the interference energy in the RF front-end and IF stages of the weather radar. Measurement results showed that interference energy originated in the unwanted emissions of the ASR (i.e., front-end overload was not occurring in the weather radar). But the problem was exacerbated by the placement of a passive diode limiter ahead of a bandpass filter in the weather radar receiver's RF front-end. The interference could not be mitigated unless the front-end configuration of the weather radar was modified. With the necessary modification completed, the interference was successfully mitigated by installing a conventional notch filter on the ASR's output stage, the notch being tuned to the weather radar frequency. It is recommended that the front-end configuration of all weather radars of the type in question should be immediately changed in the same way as the weather radar in this study, and that appropriate output filters should be installed in ASRs that are located in close proximity to these weather radars to mitigate interference effects at all sites in the U.S.

Key words: airport surveillance radar interference; radar co-channel interference; radar emission spectrum measurements; radar interference mechanisms; radar interference mitigation; Radar Spectrum Engineering Criteria (RSEC); RF front-end overload; weather radar interference

1 INTRODUCTION

When an S-band (2700-2900 MHz) airport surveillance radar was recently installed in close proximity (930 m separation distance) to a weather radar that operates in the same band, interference occurred to the weather radar. The interference caused a visible strobe to be displayed on the weather radar's diagnostic plan-position indicator screen, as shown in Figure 1. The strobe pointed in the direction of the ASR, making identification of the interference source straightforward. A solution for the interference problem was required. Since the type of solution that needs be implemented in such cases depends critically

[1] The authors are with the Institute for Telecommunication Sciences, National Telecommunications and Information Administration, U.S. Department of Commerce, Boulder, CO 80305.

upon the interference mechanism, a study was required to ascertain the type of interference and the solutions that would be viable.

This report describes the measurements and tests that were performed to determine the interference mechanism and the mitigation solutions that were determined to be appropriate. The results of tests of those solutions are presented, along with the description of a novel type of interference exacerbation that was found to result from the RF front-end configuration of the weather radar receiver.

The pertinent technical characteristics of the two radars are listed in Tables 1 and 2. Each radar tower was positioned on a hilltop, and the propagation between the antennas was line-of-sight with no obstructions between them (Figure 2). The two radar antennas were at virtually the same height relative to sea level.

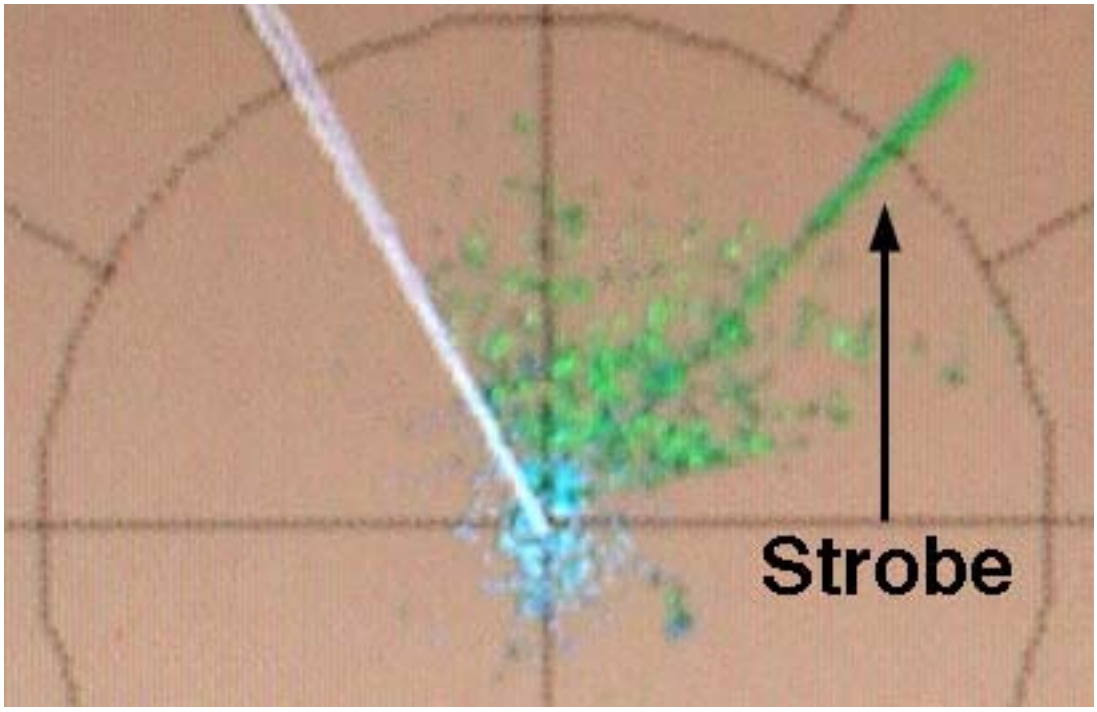

Figure 1. Photographic image of an interference strobe on the diagnostic display of the weather radar.

Table 1. Selected Technical Characteristics of the Airport Surveillance Radar.

Parameter	Value
Fundamental frequency	2860 MHz (normally used) or 2775 MHz
Transmitter type	Solid state, consisting of 8 power modules and 2 drivers
Modulations used	Interleaved unmodulated and FM-modulated (chirped) pulses
Pulse chirp width, B_c	4 MHz
Pulse sequencing	Pulses emitted in pairs, each pair consisting of an unmodulated pulse followed by an FM-modulated (chirped) pulse
Pulse widths, τ	1 μs (non-chirped); 89 μs (chirped)
Emission bandwidth	$(B_c/\tau)^{1/2} = (4\ \text{MHz}/89\ \mu\text{s})^{1/2} = 212$ kHz
Pulse intervals	105 μs between the non-chirped pulse and the chirped pulse in each pair; 1.117 ms interval from the start of one pair to the start of the next pair
Overall duty cycle	8.05 percent
Transmitter peak power	+73 dBm (20 kW)
Waveguide loss between transmitter and antenna	5 dB
Antenna gain	+34 dBi

Table 2. Selected Technical Characteristics of the Weather Radar.

Parameter	Value
Fundamental frequency	2895 MHz (35 MHz above the ASR frequency)
Pulse modulation	Pulsed Doppler
Pulse widths, τ	1.5 μs, 4.5 μs, depending upon operational mode
IF bandwidths corresponding to pulse widths	670 kHz, 220 kHz
Antenna gain	+44 dBi

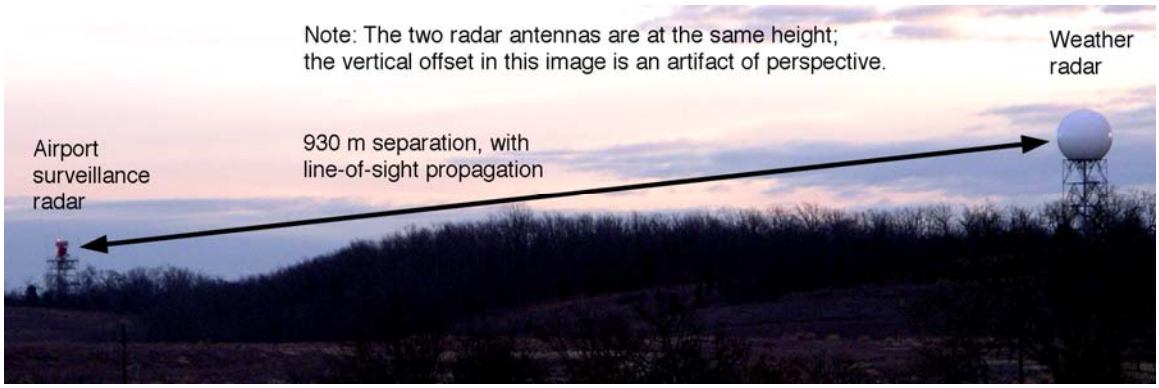

Figure 2. Radar antenna propagation geometry.

2 INTERFERENCE MECHANISMS AND DIAGNOSTICS

2.1 Interference Mechanisms

RF interference problems can be caused by a number of mechanisms, each with a corresponding mitigation technique. When considering possible solutions to a particular RF interference problem, it is essential that the type of interference mechanism that is occurring is positively identified first. For interference between radars, there are two major types of interference mechanism: front-end overload of the victim receiver low noise amplifier (LNA), and co-channel interference from the spurious or unwanted emissions of the interference-causing radar on the fundamental frequency of the victim receiver. These two mechanisms are shown schematically in Figures 3 and 4, and are described in more detail in [1].

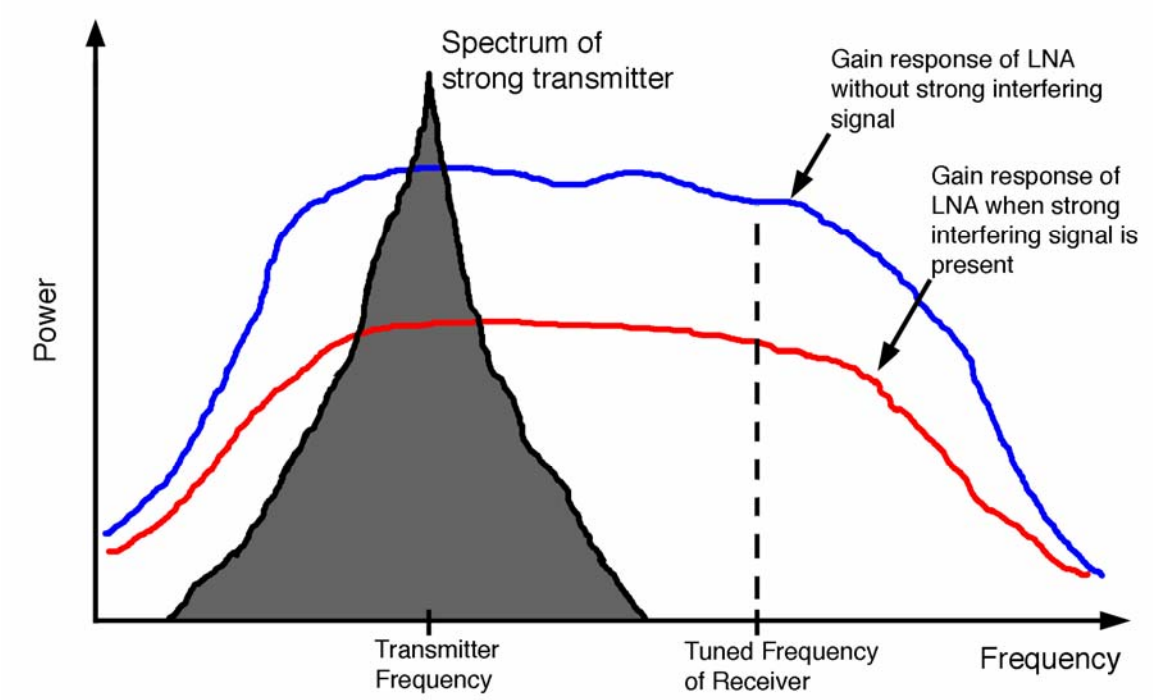

Figure 3. Schematic depiction of the front-end overload mechanism. The receiver loses its desired signal when its front-end LNA is gain-compressed by a strong signal that is far from the receiver's tuned frequency.

When front-end overload occurs, the gain of the LNA in the RF front-end of the victim receiver is driven into compression by the presence of a strong signal that is tuned somewhere within the frequency response range of the LNA. Since modern LNAs often have frequency response ranges of several gigahertz (e.g., 1-18 GHz), it is possible for the interfering signal and the victim receiver's desired (tuned) frequency to be hundreds of megahertz or even some gigahertz apart. The gain reduction in the LNA causes loss of the desired signal in the victim receiver.

Co-channel interference occurs when out-of-band (OOB) or spurious emissions (together referred to as unwanted emissions) from a radar transmitter occur on the tuned frequency of a victim receiver at a power level that is high enough to cause degradation of the victim receiver's output.

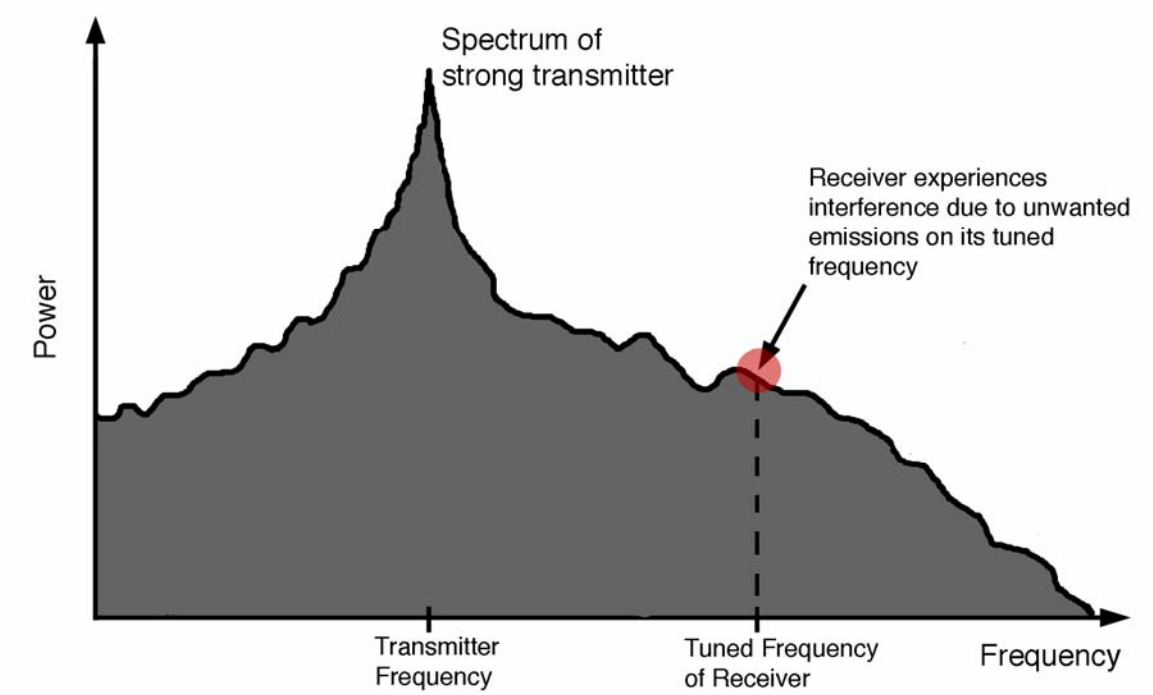

Figure 4. Schematic depiction of the co-channel interference mechanism.

Other types of RF interference exist, but they are not so easily defined as broad categories. They include such problems as inadequate grounding of the power supply or RF circuitry of the victim receiver; case penetration due to inadequate RF shielding of critical components; non-linear diode-rectification effects of incident signals near the victim receiver (the so-called rusty-bolt or rusty-fence effect); and non-linear receiver effects (other than the front-end overload effect described above) caused by poor receiver design. In this study, a receiver design problem was discovered to be a contributor to the overall interference problem, and it had to be resolved before any other mitigation solutions could be effectively implemented.

2.2 Mitigation Techniques

Filtering solutions are effective for each of the two major interference mechanisms described above, but the type and location of the filtering that must be implemented will depend critically on the type of interference that is occurring. The solutions are summarized in Table 3.

Table 3. Mitigation Solutions as a Function of Interference Mechanism.

Interference Mechanism	Mitigation Solution
RF front-end overload (due to lack of bandpass filtering in the *receiver*)	Bandpass filter installation on the victim *receiver* RF front-end
Co-channel (due to unwanted emissions from the *transmitter*)	Notch, highpass, or lowpass filter installation on the *transmitter*
Other categories referred to in the text	Various, innovative solutions depending upon the problem

The critical difference between the solutions for the two major interference mechanisms is that RF front-end overload interference can be mitigated *only* by installing bandpass filtering on the RF front-end of the *victim receiver*. Co-channel interference, in contrast, can be mitigated *only* by installing filtering (usually either notch, highpass, or lowpass) on the output stage of the *transmitter* that is generating the interfering energy.

2.3 Diagnostics for Interference Mechanisms

Given the criticality of identifying the interference mechanism that is occurring so that the proper solution can be tested most efficiently (and that valuable time and effort not be wasted on mitigation approaches that will not work), it is essential to understand the observations that must be performed to identify the interference mechanism that is occurring. These observations are described in detail in [1], and are summarized here from that source.

2.3.1 RF Front-End Overload Diagnostics

The diagnostic observation for RF front-end overload due to radar pulses is gain compression behavior of the front-end LNA. This effect can be observed in the time domain at the LNA output, and also in the IF stage of the victim receiver (assuming that the LNA excess noise output determines the receiver noise level in the IF stage). This behavior is manifested as a decrease in the noise floor of the LNA, and is easily observed with a spectrum analyzer. An example of this effect is shown in Figure 5 (extracted from [1]).

In Figure 5, an LNA was subjected to high-amplitude inputs from a pulsed signal source in a laboratory, and its responses were measured as a function of interference amplitude. The result was a series of curves showing gain compression and recovery as a function of interference amplitude. On these curves, interference pulses are injected at time t=0 and the gain response is compressed to greater and greater degrees as interference amplitude increases. The gain compression is observed as a decrease in the LNA output noise by amounts ranging from 10 dB to 40 dB. Subsequently, the LNA gradually recovers over time intervals that range from 100 μs to 900 μs. Other LNAs will exhibit quantitative variations on this response, as documented in [1], but qualitatively the overload effects will always be the same as those shown in Figure 5.

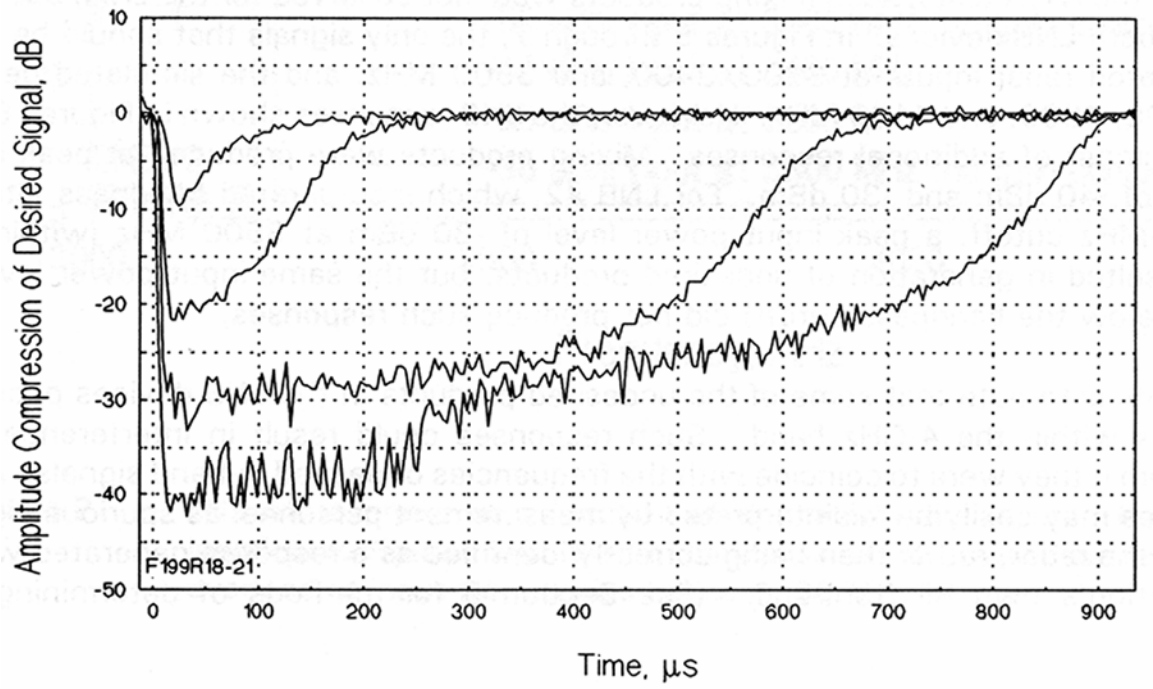

Figure 5. Example of gain compression at an LNA output for varying levels of overload.

2.3.2 Co-channel Interference Diagnostics

The diagnostic observation for co-channel interference due to radar unwanted emissions is ragged or irregular pulse shapes, as measured on the victim receiver's frequency. The physical phenomenon is as follows. When a measurement of pulse shape is performed at the fundamental frequency of a pulsed source (such as a radar), the Fourier lines convolved by the measurement filter will produce a good approximation of the nominal pulse shape envelope in the time domain. An example of this behavior is shown in the top row of Figure 6 for long-pulse and short-pulse modes of a radar transmitter.

However, when the same measurement filter is tuned to any given frequency in the unwanted (OOB or spurious) portions of the pulsed-emission spectrum, the Fourier lines that it convolves will fail to produce a smooth, clean pulse shape envelope in the time domain. Instead, the observed pulse envelopes will either appear ragged, as shown in the lower right-hand corner of Figure 6, or else will exhibit a pair of spikes (with a spacing equal to the nominal pulse width), as shown in the lower left-hand corner of Figure 6.

When a victim receiver is affected by co-channel interference due to unwanted emissions from a radar, its bandpass characteristic will convolve a subset of Fourier lines in the portion of the interferer's spectrum that corresponds to its tuned frequency. The result will be that the interference pulses at either the receiver's LNA output or the victim receiver's IF stage will have the same appearance as the pulse envelopes in the lower row of Figure 6. More details on the physics of this phenomenon are provided in [1].

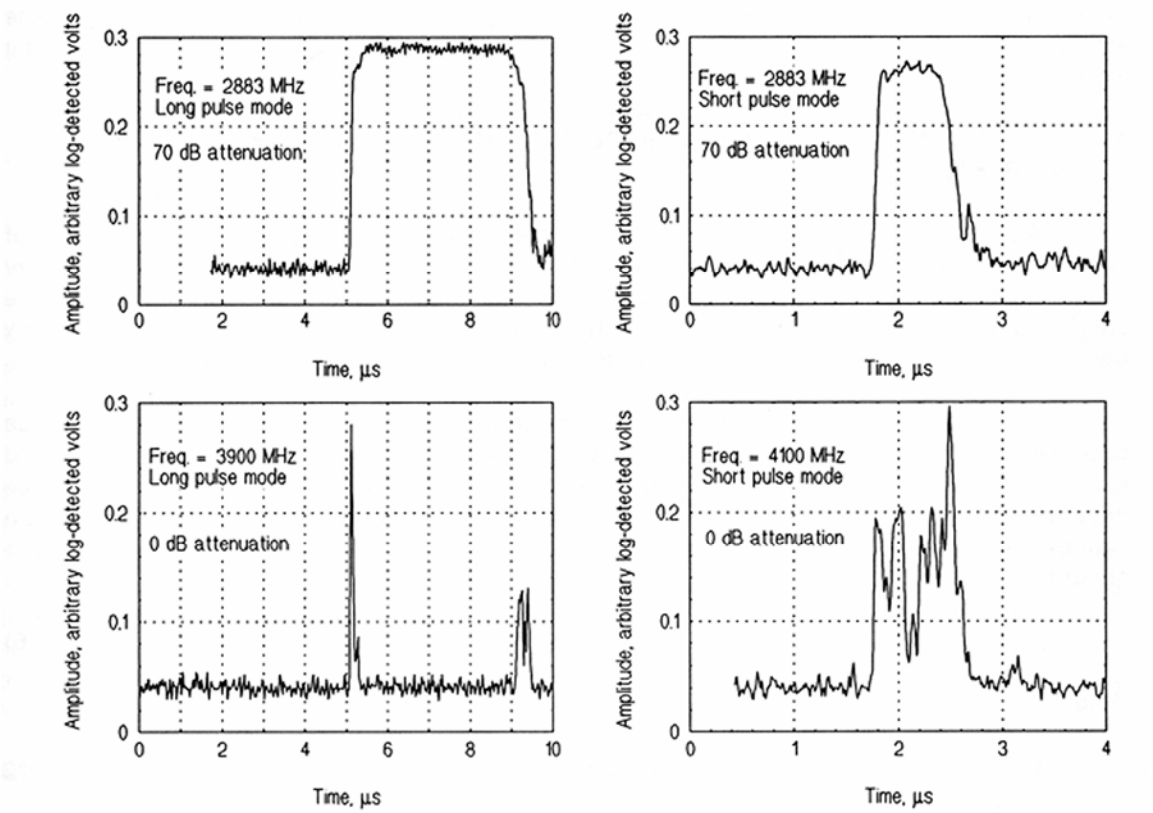

Figure 6. Examples of comparative pulse shapes at a radar fundamental frequency in long pulse and short pulse modes (left and right, respectively, in the upper row), versus examples of the corresponding pulse shapes that are observed at off-tuned frequencies in the unwanted emission spectrum in the same modes (lower row). The ragged, or 'rabbit ears' shapes of the pulses at the off-tuned measurement frequencies are the result of measurement bandwidth-limiting of the Fourier lines in the radar unwanted emission spectrum.

2.4 Measurements to Determine Interference Mechanism

Given the clear-cut differences between the two types of interference mechanisms, the observations that need to be performed to determine which mechanism is occurring are straightforward. At the output of the LNA in the receiver's RF front-end, or else (or in addition) in the IF stage of the victim receiver, the interference pulses should be observed in the time domain. In particular, the pulse envelopes should be resolved. Inspection needs to be performed for the presence of gain compression (such as depicted in Figure 5) in the intervals immediately following the interference pulses, and the pulse envelopes should be inspected for a ragged or double-spiked (so-called rabbit ears) appearance, as depicted in Figure 6. Depending upon which effect is observed, the interference mechanism is diagnosed and the method for resolving the problem is as specified in Table 3.

In the event that neither effect is observed, it is likely that some sort of non-linear behavior is occurring in the victim receiver, and the receiver's design and construction need to be examined for possible sources of such behavior. As will be seen, such an effect was found to occur in the course of this case study.

2.5 Supporting Measurements

Additional measurements need to be made when interference is caused by a radar transmitter (i.e., co-channel interference due to a radar's unwanted emissions). In particular, the emission spectrum of the radar that is suspected as the source of interference needs to be measured to determine whether it complies with applicable emission mask limits. For radar transmitters inside the U.S., the NTIA Radar Spectrum Engineering Criteria (RSEC), as described in [2], describe the applicable mask limit. Conformance with the RSEC mask limit by a radar's emissions does *not* guarantee that interference will not be caused by that radar's unwanted emissions. But conformance versus non-conformance with the mask may be an important factor in determining which entities may be responsible for providing the necessary resources to filter the emissions of the radar in question.

When such emission spectrum measurements need to be performed, the procedures given in [3] should be followed. The emission measurements need to be performed on radiated energy from the transmitter, rather than through hardline coupling from the transmitter.[2] Selection of the proper measurement bandwidth is absolutely critical. For transmitters with unmodulated pulses, the proper measurement bandwidth is less than (1/pulse width). For chirped-pulse emissions, the proper measurement bandwidth is less than $(B_c/\tau)^{1/2}$, where B_c = chirp bandwidth and τ = pulse width. See [3] for additional information about proper measurement bandwidths, measurement algorithms, measurement system hardware design, and other critical aspects of RSEC-compliance measurement techniques.

In addition to the radar emission spectrum, the radar pulse waveforms, pulse repetition sequence, and antenna pattern should all be measured and recorded as described in [3].

2.6 Approach to Measurements

Given the goals for measurements and diagnostic observations as outlined above, the overall approach that is most often successful is to measure the interfering energy beginning with the radiation from the transmitter that is thought to be causing interference. Then the energy from that transmitter needs to be traced through the victim receiver starting at its antenna output, progressing through each stage of its RF front-end after the antenna, and then continuing to trace the energy through its IF stages up to the detector (or equivalent signal-processing terminal point). At each of these stages, the

[2] Hardline-coupled measurements have been found to contain modes that do not occur in radiated emissions. See [3] for more details on the trade-offs between radiated and hardline-coupled measurements.

spectrum and time waveform characteristics of the interfering energy need to be measured, with care given to thorough documentation. The diagnostics described above for front-end overload and co-channel interference need to be applied at each stage.

Although unexpected behaviors may occur in the victim receiver, as described in this case study, this approach should nevertheless ultimately yield a successful conclusion to the effort to determine the interference mechanism and resolve the interference problem. Unexpected behaviors, if any occur, will inevitably be revealed by carefully tracing the interfering energy through the stages of the victim receiver.

3 ON-SITE INTERFERENCE RESOLUTION MEASUREMENTS

On-site interference resolution measurements were performed at Ft. Smith, Arkansas January 24-26, 2006. The purpose of the measurements was to ascertain the interference mechanism and implement one or more solutions for the problem. Broadly, the measurement sequence was as described in Section 2.6. Emission spectrum and time waveform measurements were performed on the radiated energy from the airport radar, and then the spectrum and time waveforms of the energy from the airport radar were measured inside the RF front-end and IF stages of the weather radar. The diagnostic criteria described in the previous section were used to ascertain the interference mechanism, as well as likely solutions. This section describes the interference resolution measurements and their results.

3.1 Measurements of the Airport Radar's Radiated Emissions

The NTIA/ITS Radio Spectrum Measurement System, fourth generation (RSMS-4), as shown in Figure 7, was used to perform radiated emission spectrum and time waveform measurements on the airport radar.

Figure 7. NTIA/ITS RSMS-4 vehicle. Major elements include an RF-shielded equipment enclosure, two telescoping masts, and an on-board power generator.

For these measurements, the RSMS was positioned on the same hilltop as the weather radar, where clear line-of-sight propagation was available to the airport radar antenna. The separation distance between the RSMS and the radar was determined with a laser range finder to be 489 m (530 yds).

The measurements proceeded in accordance with the techniques specified in [3]. Two independent measurement systems, one that had been used for many years and another that was new, were used to gather data. Each measurement system consisted of a 1-m

diameter parabolic dish antenna, a low-noise, frequency-selective RF front-end, a spectrum analyzer, and a controller computer. Figure 8 shows a block diagram of the measurement system RF front-ends. It is emphasized this design for a measurement system is absolutely essential for successful and accurate measurements of radar emission spectra, as described in [3]. The emission spectrum measurement rate was accelerated by halting the rotation of the airport radar antenna and boresighting it directly on the RSMS location.

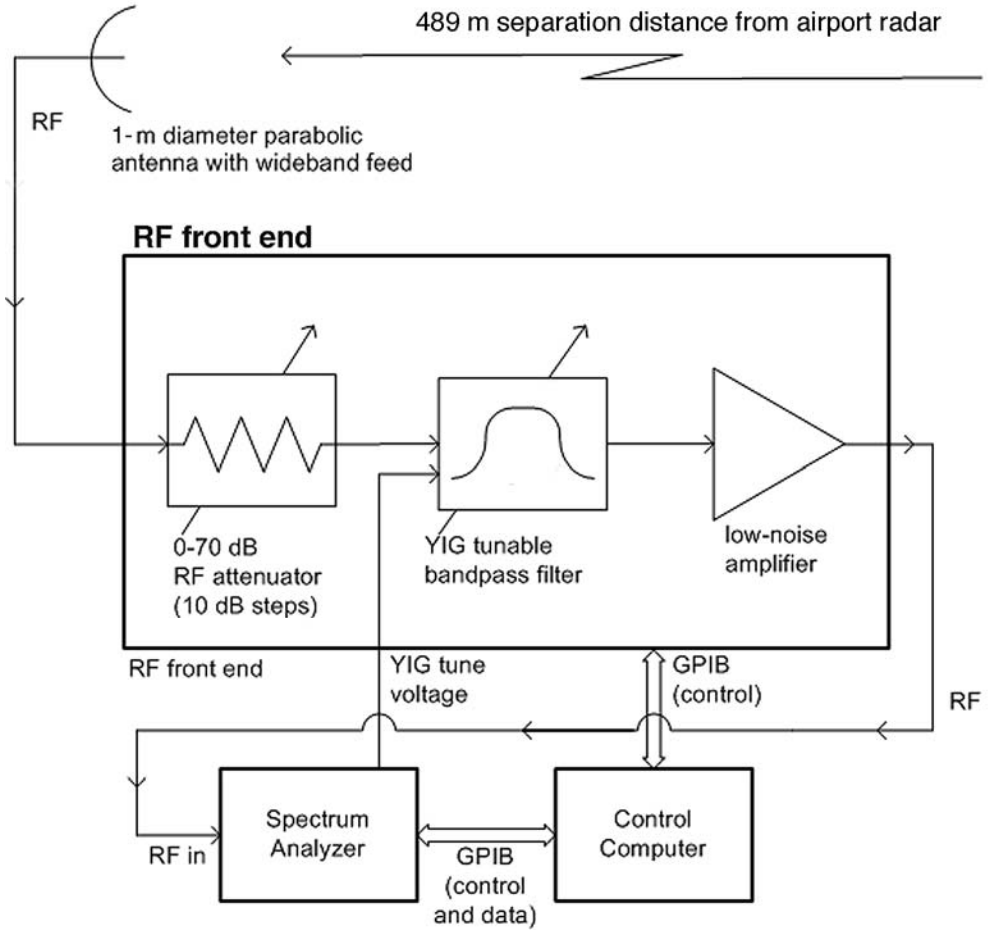

Figure 8. Block diagram of radar spectrum measurement system, based on ideal design given in [3].

The measurements were performed in several bandwidths, and two of those bandwidths in particular were 680 kHz and 200 kHz. Each of these bandwidths corresponded to one of the IF bandwidths of the victim receiver. By coincidence, the 200 kHz bandwidth also happened to be nearly the same as $(B_c/\tau)^{1/2}$, the ideal measurement bandwidth for the RSEC compliance measurement for this radar (computed as 212 kHz in Table 1). Thus two measurement bandwidths satisfied three measurement needs. The results of the spectrum measurement are shown in Figure 9.

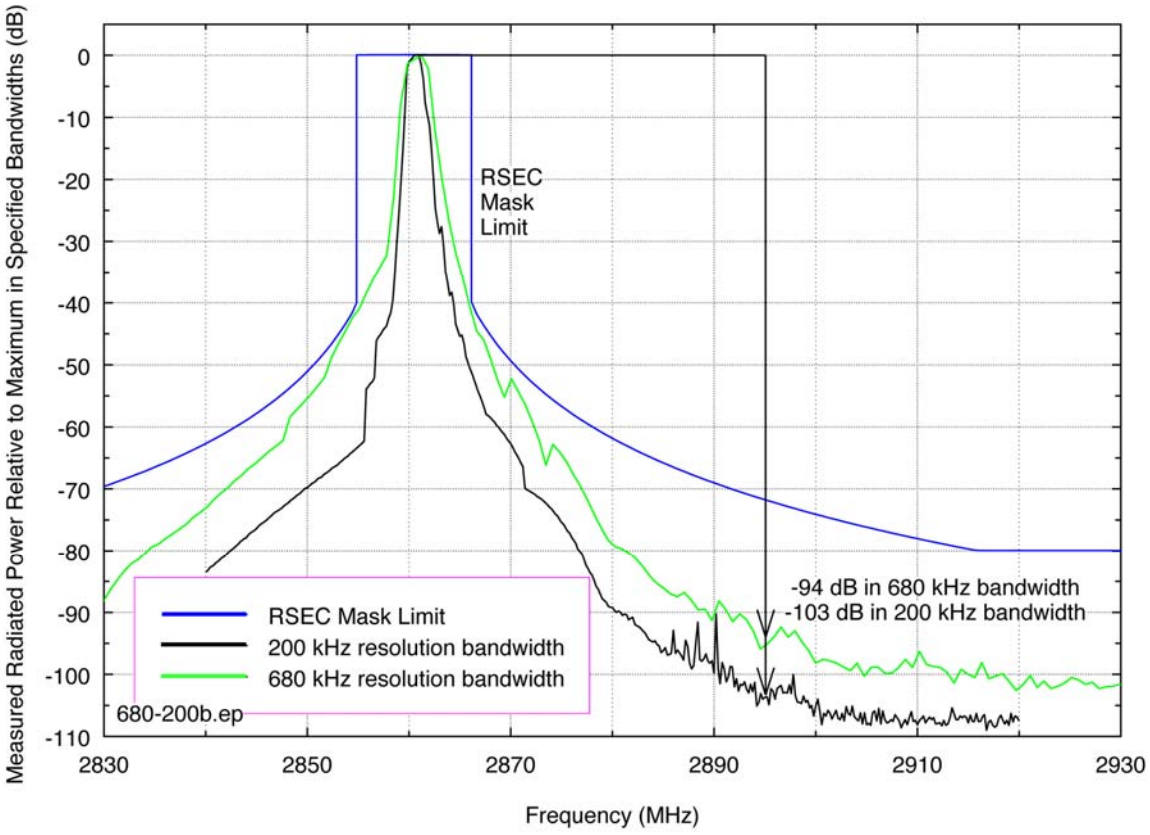

Figure 9. Radiated emission spectra of the airport radar with RSEC mask.

As shown in Figure 9, the radiated emission spectrum levels at the frequency of the weather radar (35 MHz above the frequency of the airport radar) are -94 dB relative to the radiated power level at the fundamental in the 680 kHz bandwidth, and -103 dB relative to the radiated fundamental power level in the 200 kHz bandwidth. The roll-off rate seen in Figure 9 is considered to be good compared to emission spectra that have been measured from other radars with a similar mission and design. It is noted that the 110-dB dynamic range of the measured spectrum in Figure 9 is only achievable with the kind of measurement system hardware and software that were used at this location, as described in [3].

Based on a pulse rise time measurement (radiated) of 0.15 μs, a pulse width of 89 μs, a chirp range of 4 MHz, and a roll-off rate of 40 dB per decade, the RSEC emission mask is as drawn in Figure 9. The mask applies to the data taken in 200 kHz. The radar emission meets the RSEC emission mask limit.

Figure 10 shows the time waveform envelope that is emitted by the airport radar. The pulses occur in pairs spaced 1.117 ms apart. Each pair consists of a 1-μs, unmodulated pulse followed by an 89-μs pulse that is chirped across 4 MHz of bandwidth.

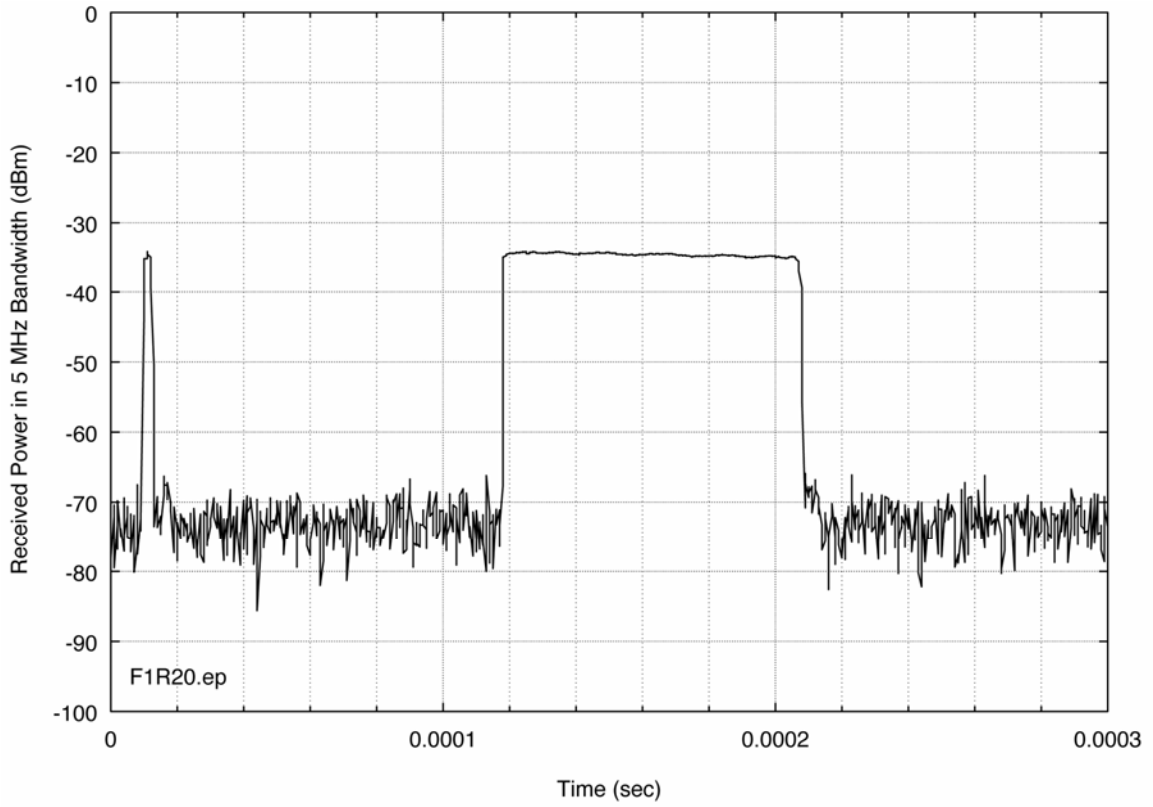

Figure 10. Detected time waveform envelopes of a radiated pair of airport radar pulses. The first pulse is unmodulated, and the second is FM-modulated (chirped).

3.2 Measurements Inside the Weather Radar RF Front-End

Figure 11 shows a highly simplified block diagram schematic of the weather radar receiver; monitoring points are noted in that diagram. RF protection was provided in the front end by a passive diode limiter (PDL) and an electromagnetic interference (EMI) bandpass filter, shown in Figures 12 and 13, respectively.

The spectrum at the outputs of the weather radar antenna front-end 20-dB coupler and passive diode limiter (PDL) are shown in Figures 14 and 15, respectively. Nothing surprising was noted in these spectra. But when the spectrum was measured at the output of the EMI filter, the curve of Figure 16 was observed. This result was surprising, as indicated by the superposed curves of the PDL and EMI output spectra (from Figures 15-16) in Figure 17.

It was concluded that a non-linear interaction was occurring between the PDL and the EMI filter, such that when the PDL was connected to the EMI filter input, and high-amplitude interference energy was injected into the PDL, the result was a non-linear output at the EMI filter output. The injected energy level of +5 dBm at 2860 MHz was redistributed across a wide spectrum range (at a density of -25 dBm in the measurement bandwidth), illuminating the bandpass shape of the EMI filter (and limited by that bandpass, as shown in Figures 16-17).

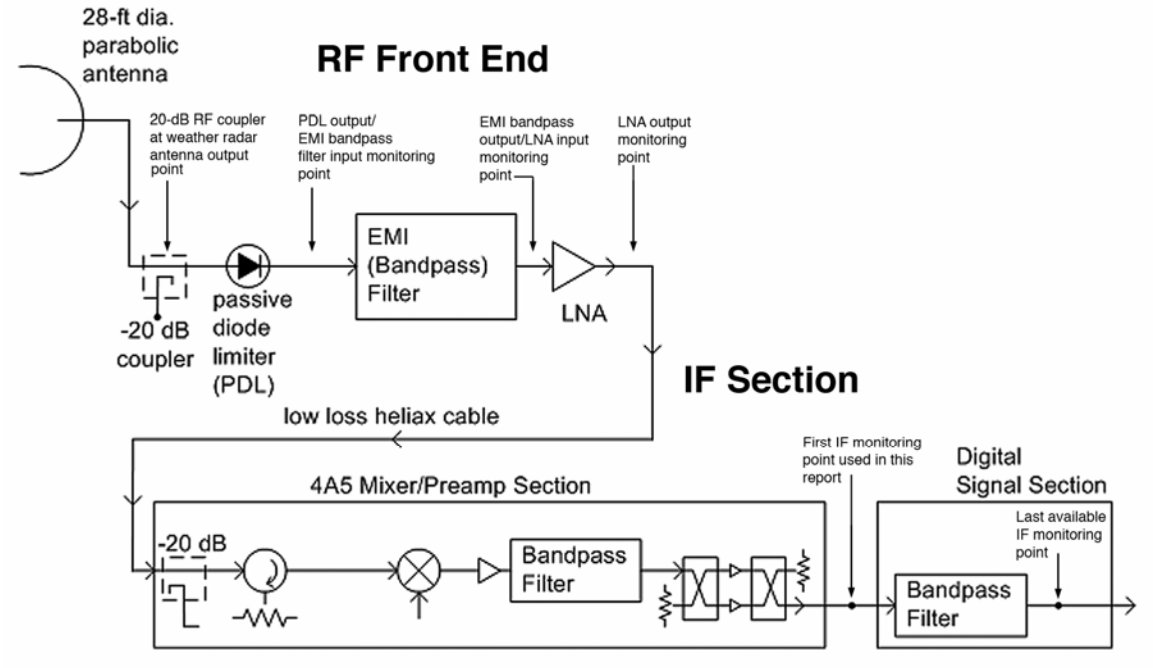

Figure 11. Simplified block diagram schematic of the weather radar receiver.

Figure 12. Weather radar receiver passive diode limiter.

Figure 13. Weather radar receiver EMI bandpass filter.

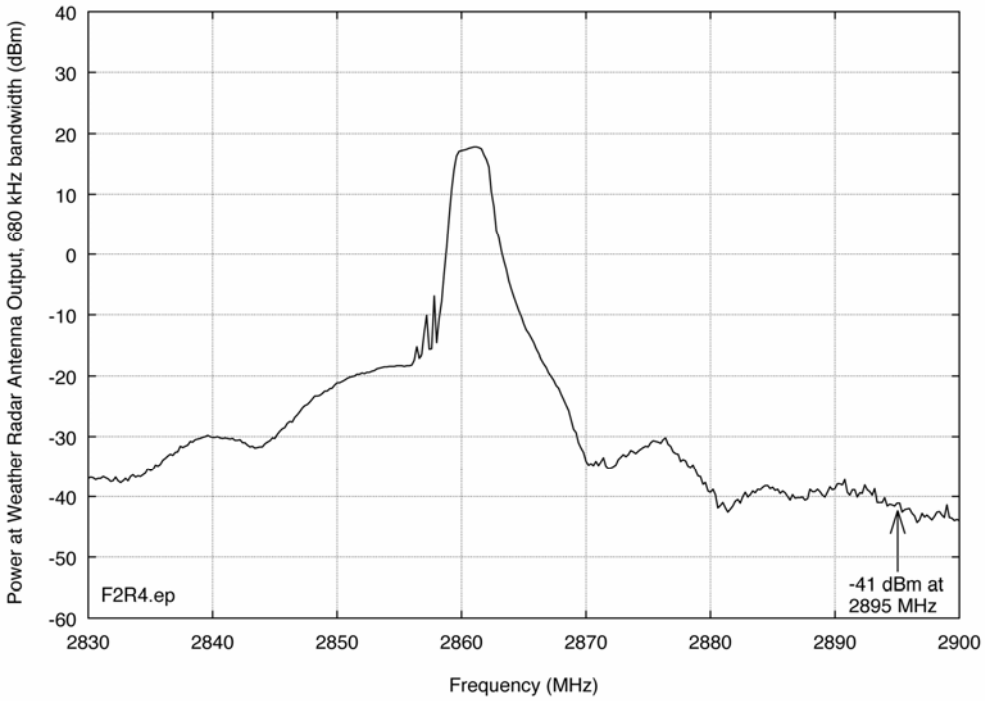

Figure 14. Airport radar spectrum measured through the weather radar receiver's RF front-end 20-dB coupler.

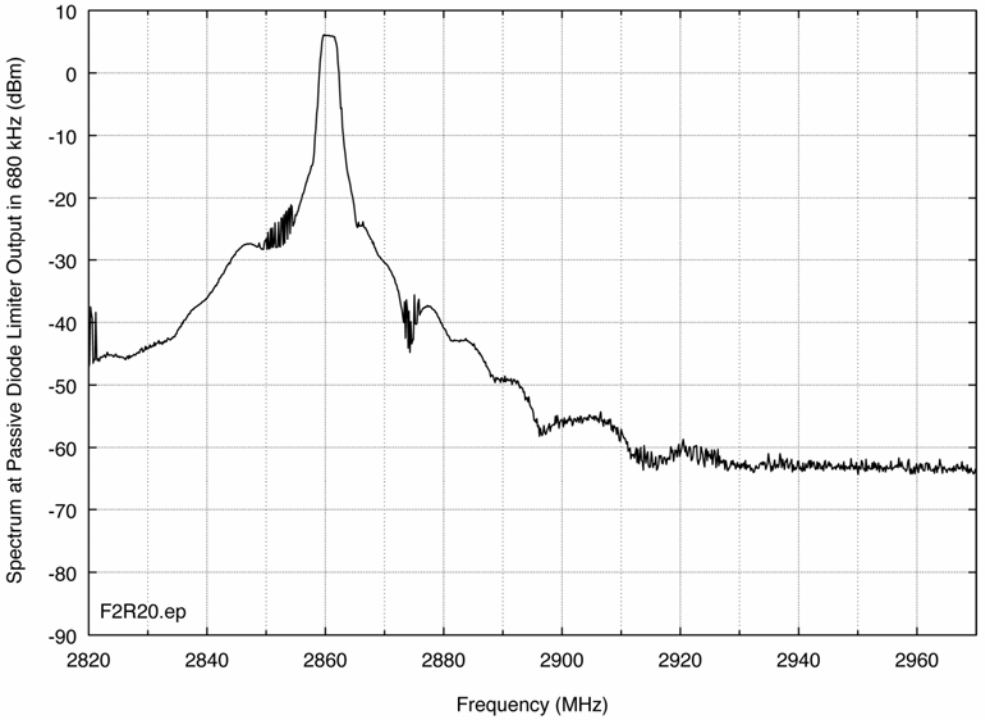

Figure 15. Airport radar spectrum measured at the output of the passive diode limiter. Nothing surprising had been noted up to the point that the spectrum was measured at the output of the PDL. But when the spectrum was measured at the output of the electromagnetic interference suppression bandpass filter (EMI filter), the result was as shown in the next figure (Figure 16).

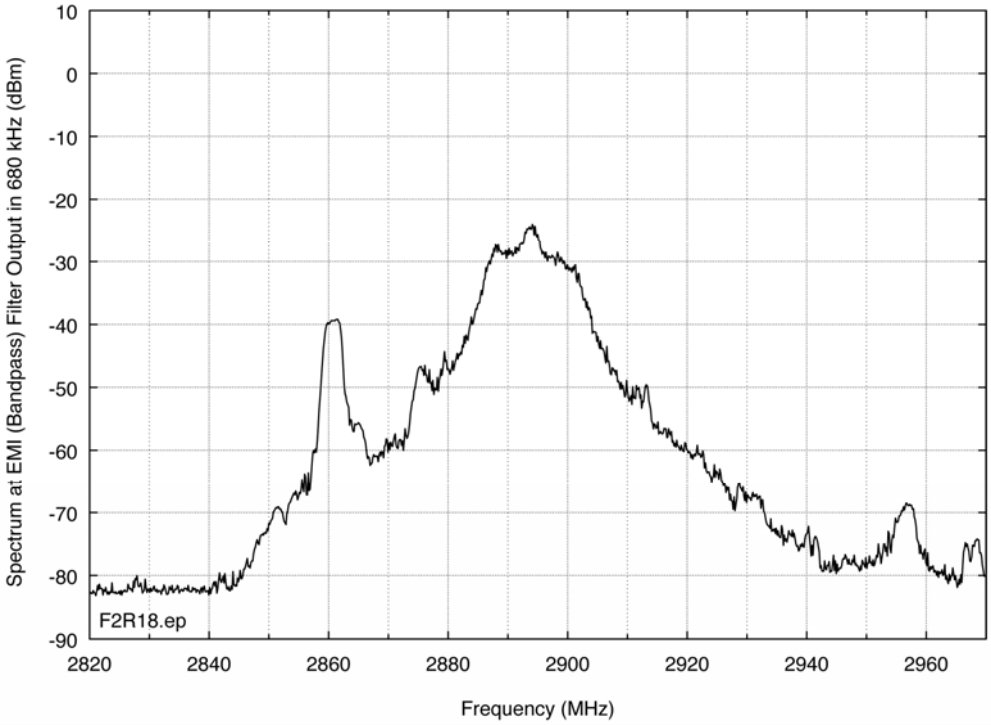

Figure 16. Spectrum measured at output of EMI filter. This should have looked like a band-limited version of the curve in Figure 15, but it did not.

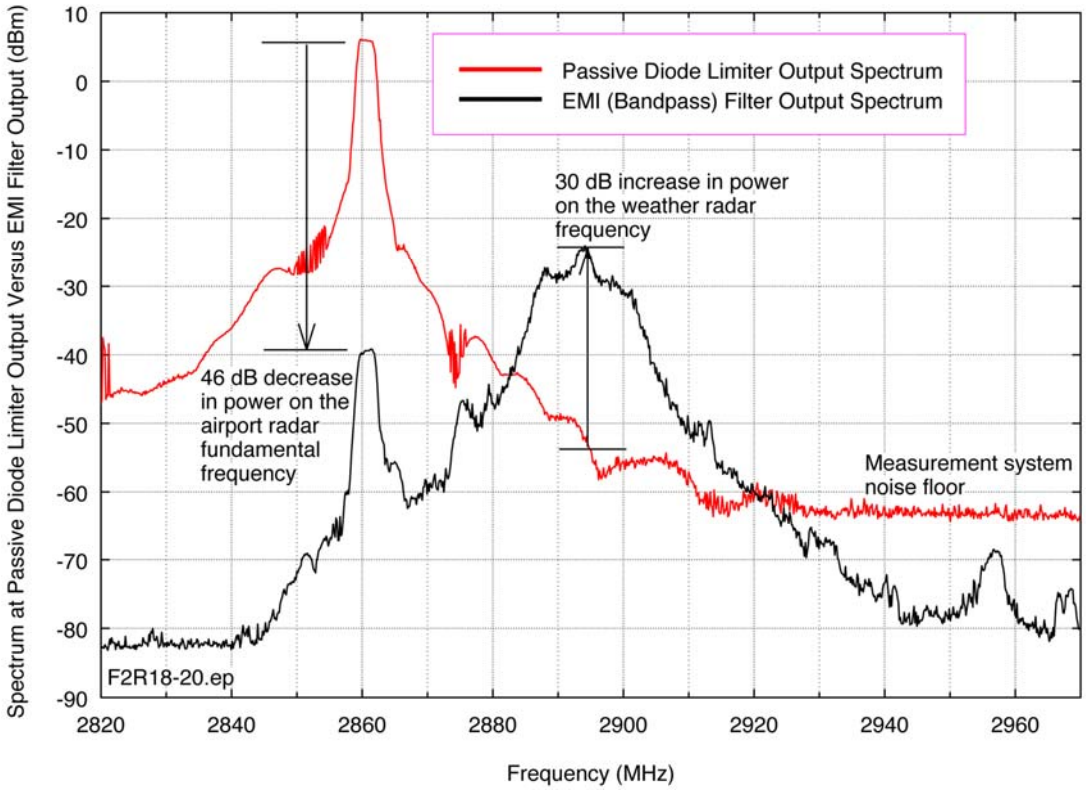

Figure 17. PDL and EMI output spectra overlaid on each other, from Figures 15 and 16.

To ascertain the nature of the effect, the PDL was removed from the system and the spectrum was again measured at the output of the EMI filter, the result being shown in Figure 18. Then the PDL was reintroduced into the system immediately *after* the EMI filter. The resulting spectrum for this configuration at the PDL output is shown in Figure 19. The results obtained when the PDL was removed entirely versus when the PDL was placed after the EMI filter were nearly identical. In Figure 20, all of the curves from the previous set of figures are overlaid to demonstrate more clearly the relationships between the results obtained for all of these configurations.

The explanation for this behavior probably lies in the way that PDL's are supposed to operate. In principle, a PDL output should be connected to the input of an LNA to prevent physical damage to the LNA due to high-power signals. The PDL output impedance is ordinarily supposed to be high. But when the PDL is subjected to a signal power level that exceeds a certain threshold, the PDL output impedance is supposed to go to a low value, as close to zero as possible. The impedance change should then cause the high-power signal to be reflected backward out of the PDL's (nominal) input port. In effect, the PDL is supposed to function like a fast-response, pop-up electromagnetic mirror.

In reality, when the PDL output was connected to the EMI filter input, the PDL output impedance may not have dropped as low as desired. As a result, when high energy levels impinged on the PDL, some of that energy was still passed forward (with a wideband spectrum distribution). This non-linear response was eliminated by moving the PDL to a location *after* the weather radar EMI filter. The response of the LNA to the energy from the airport radar was as shown in Figure 21.

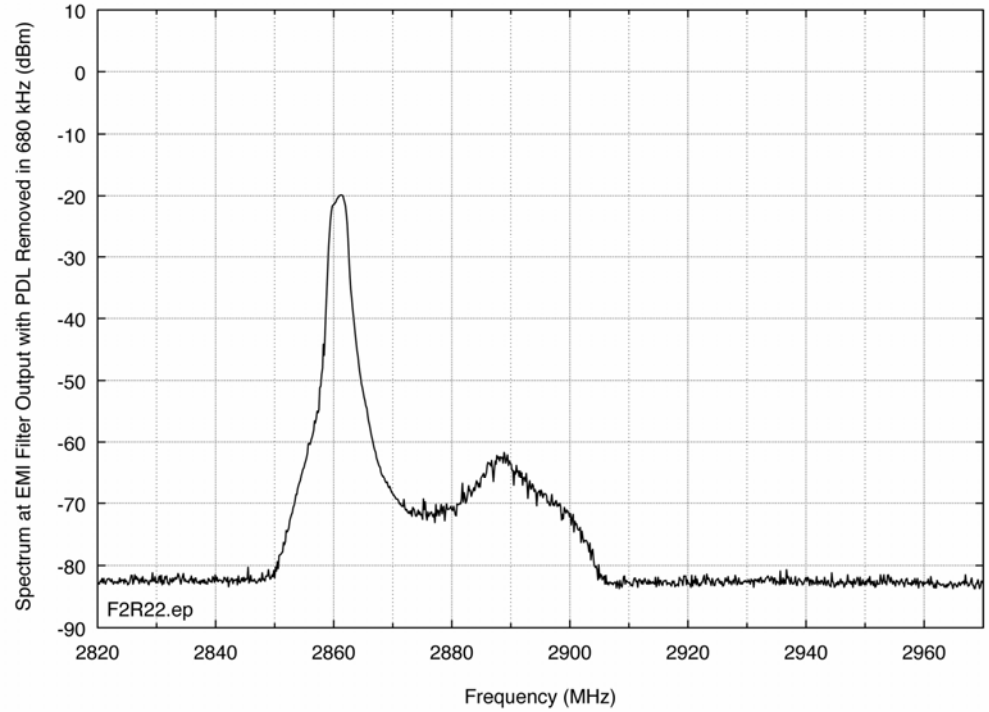

Figure 18. Spectrum at EMI filter output when the PDL was removed from the system.

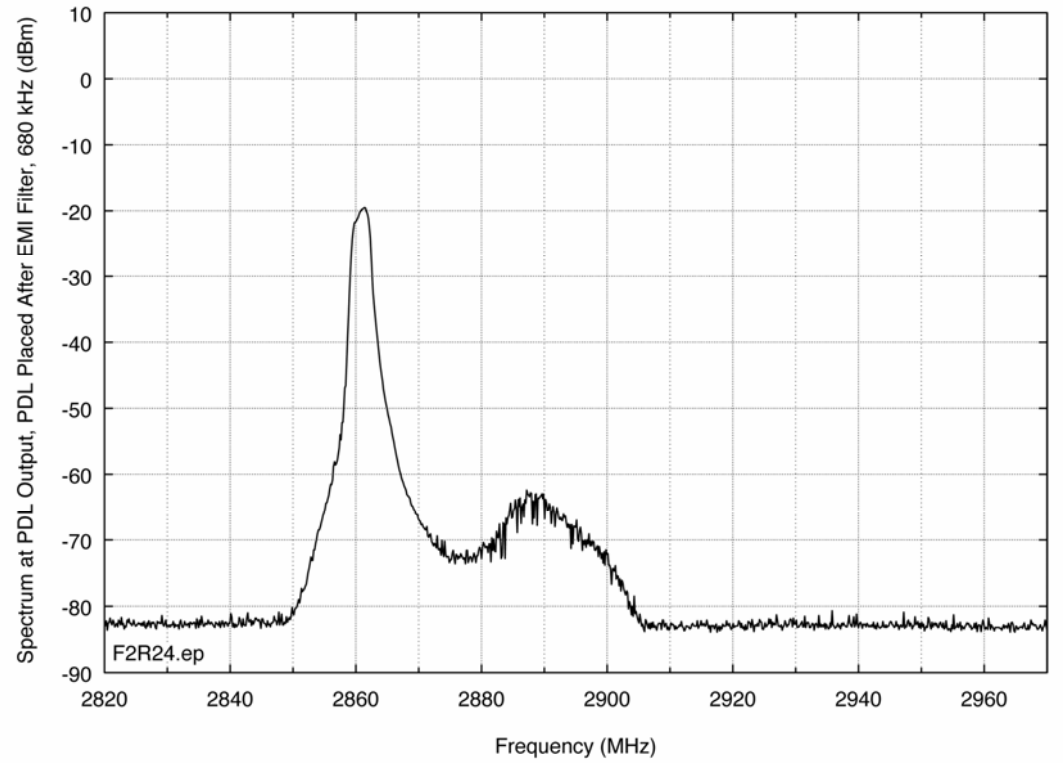

Figure 19. Spectrum at PDL output when PDL was placed *after* the EMI filter; the result is virtually identical to the data curve of Figure 18.

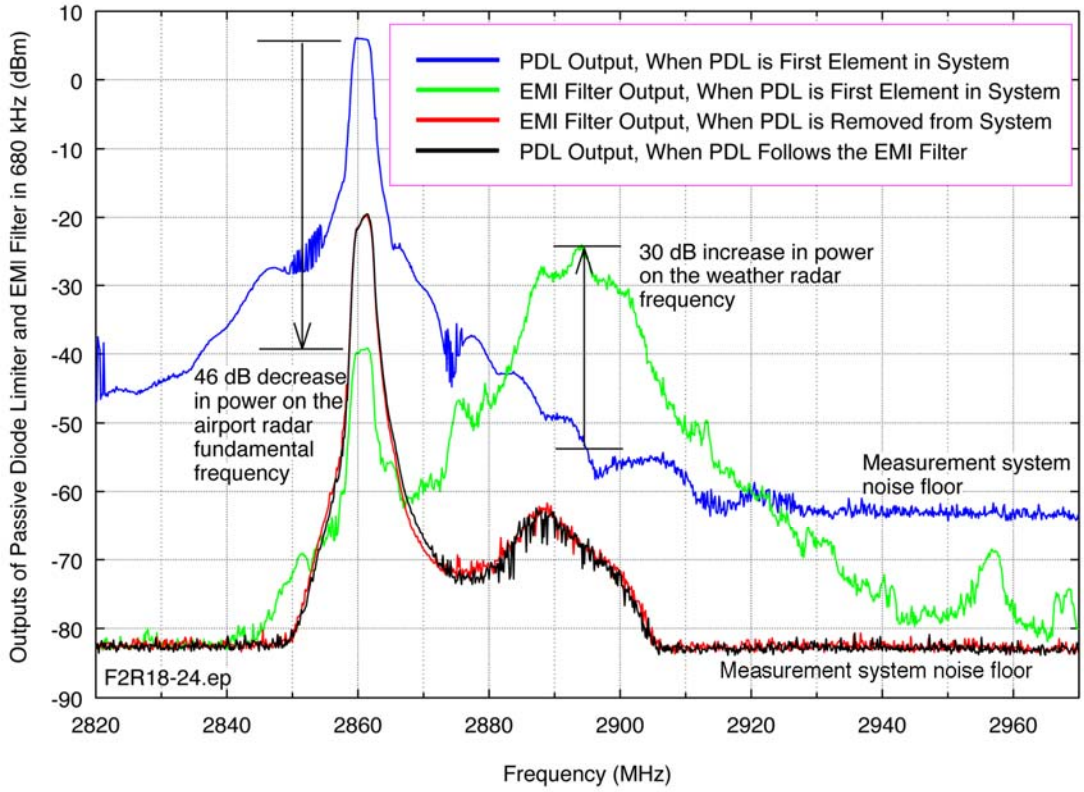

Figure 20. Comparative results for various PDL and EMI configurations.

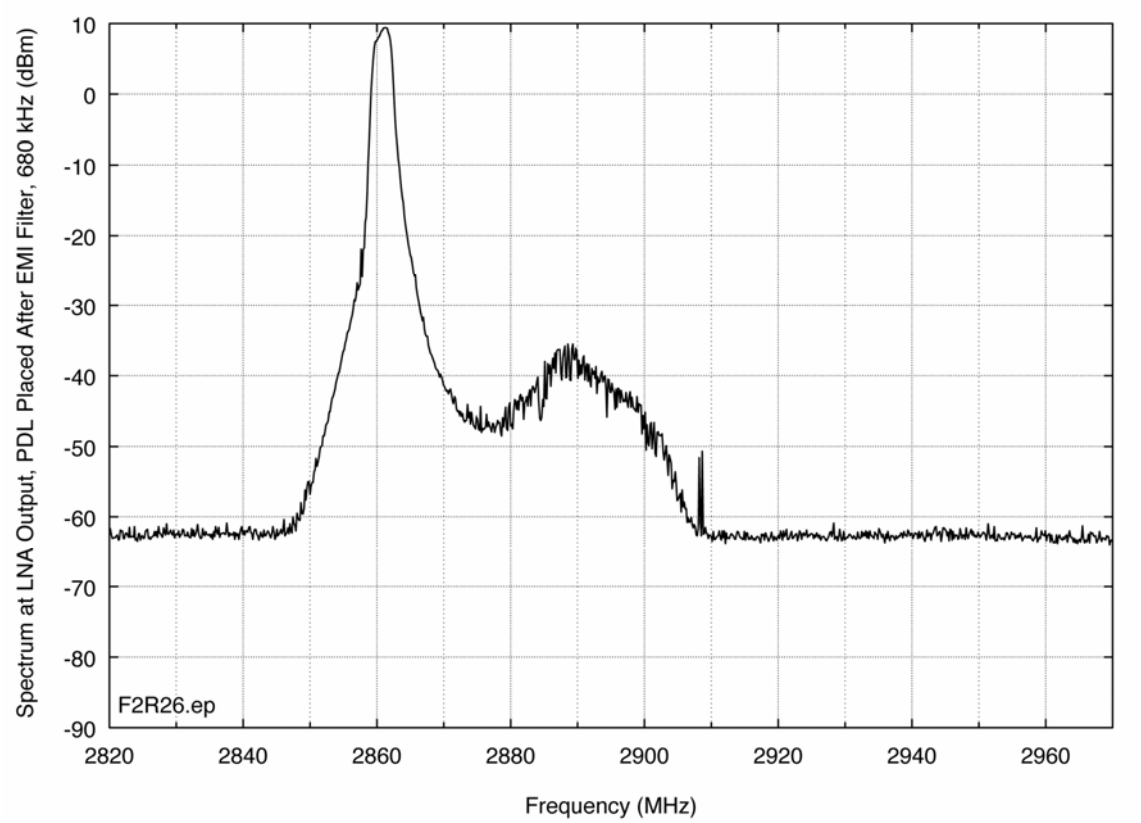

Figure 21. Response of the LNA to the airport radar energy when the PDL was placed after the EMI filter.

Even when the PDL was in its original location, ahead of the EMI filter, time-domain pulse envelope waveforms showed no indication of front-end overload, as shown in Figure 22. In this figure, *neither* front-end overload gain compression *nor* the ragged, rabbit-ears envelopes of unwanted emissions are observed—a seemingly paradoxical result that could not be resolved until the non-linear behavior of this front-end configuration was understood. This paradox had apparently confounded previous attempts to resolve the interference problem between these radars.

With the non-linear front-end combination in place (that is, with the PDL in front of the EMI filter), the power injected into the LNA input, as high as it was, was still not sufficient to push the LNA into gain compression. But the time waveform going into the LNA and being amplified was *not* that of the airport radar's unwanted emissions occurring on the weather radar fundamental frequency. Instead, the airport radar's *fundamental frequency* energy (separated by 35 MHz from the weather radar receiver's tuned frequency) was spectrally redistributed inside the weather radar receiver's RF front-end across a range of frequencies that included the weather radar fundamental frequency. That was the effect of the non-linear element, the PDL, acting at the input port of the EMI bandpass filter.

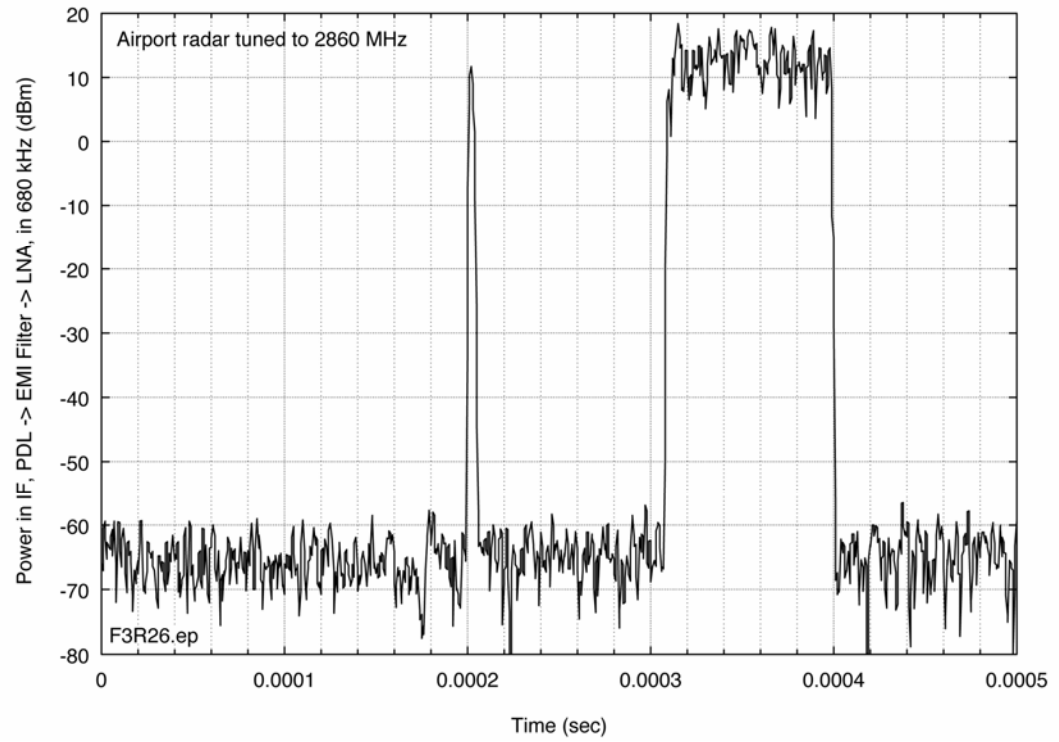

Figure 22. Time domain waveform at the output of the LNA when the PDL was located in its original position, in front of the EMI filter.

Until this effect was finally understood, any attempts to resolve the interference problem would be futile. For example, the installation of any sort of filter on the output of the airport radar would have been completely ineffective.

Other than moving the PDL behind the EMI filter (or removing it from the system entirely), only one other technical solution was possible: To place a notch filter in front of the PDL, the notch frequency being tuned to the fundamental frequency of the airport radar. This experiment was tried, and the resulting spectrum is shown in Figure 23.

With the notch filter in place, the LNA output spectrum was the same as when the PDL was either removed entirely or was placed behind the EMI filter. But this would not be considered a satisfactory solution for the weather radar, inasmuch as the insertion loss of the notch, which was several decibels, would add directly to the noise figure of the weather radar and would be expected to considerably degrade its performance. In the end, the notch filter experiment served mainly to confirm that the PDL must not be allowed to experience a high input signal level, lest it interact with the EMI bandpass filter in such a way as to generate the output of Figure 16.

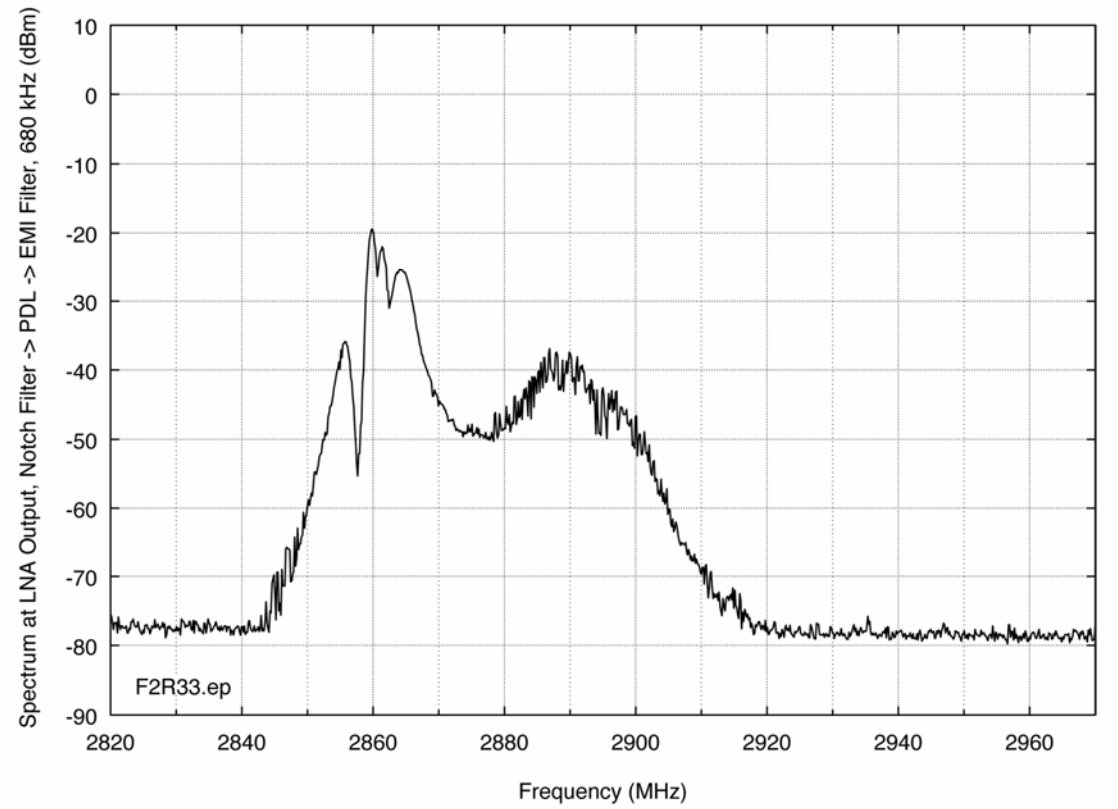

Figure 23. Spectrum at LNA output when a notch filter was placed in front of the PDL. The PDL was in its normal location in front of the EMI filter.

3.3 Measurements Inside the Weather Radar IF Stage

With the non-linear behavior in the RF front-end understood, and no indication at the LNA output that front-end overload was occurring (even with the non-linear behavior, much less when the non-linear behavior was corrected), the next step was to perform measurements within the IF stage of the weather radar. Figure 24 shows the radar IF spectrum when no interference was present (i.e., when the airport radar transmitter was turned off), as measured at the "first available IF monitor point used in this report" shown in Figure 11.[3, 4] This spectrum was generated with a peak detector; the RMS average noise level would have been about 10 dB lower.

[3] Subsequent IF-stage measurements were also performed at this point, unless otherwise indicated.

[4] It is noted that the average level of the weather radar noise floor is -80 dBm; the IF noise floor observed in Figure 24 is peak-detected rather than average, and has not been corrected for the receiver's gain at that point. The level shown in Figure 24 is used only as a reference for the data shown in subsequent figures (such as Figure 30) in this report.

Figure 25 shows the weather radar IF spectrum with the same measurement configuration as for Figure 24, but when the airport radar transmitter was radiating. The RF front-end was configured in its non-linear combination, with the PDL ahead of the EMI filter. Here, the interference level is about 85 dB higher than the IF noise level from the previous figure.

In Figure 26, the weather radar IF spectrum is shown when the PDL was placed *after* the EMI filter; Figure 27 overlays these curves for comparison. When the PDL was placed after the EMI filter, the interference to noise (*I/N*) ratio in the weather radar IF stage was reduced by about 45 dB relative to the level in Figure 26, with the original front-end configuration.

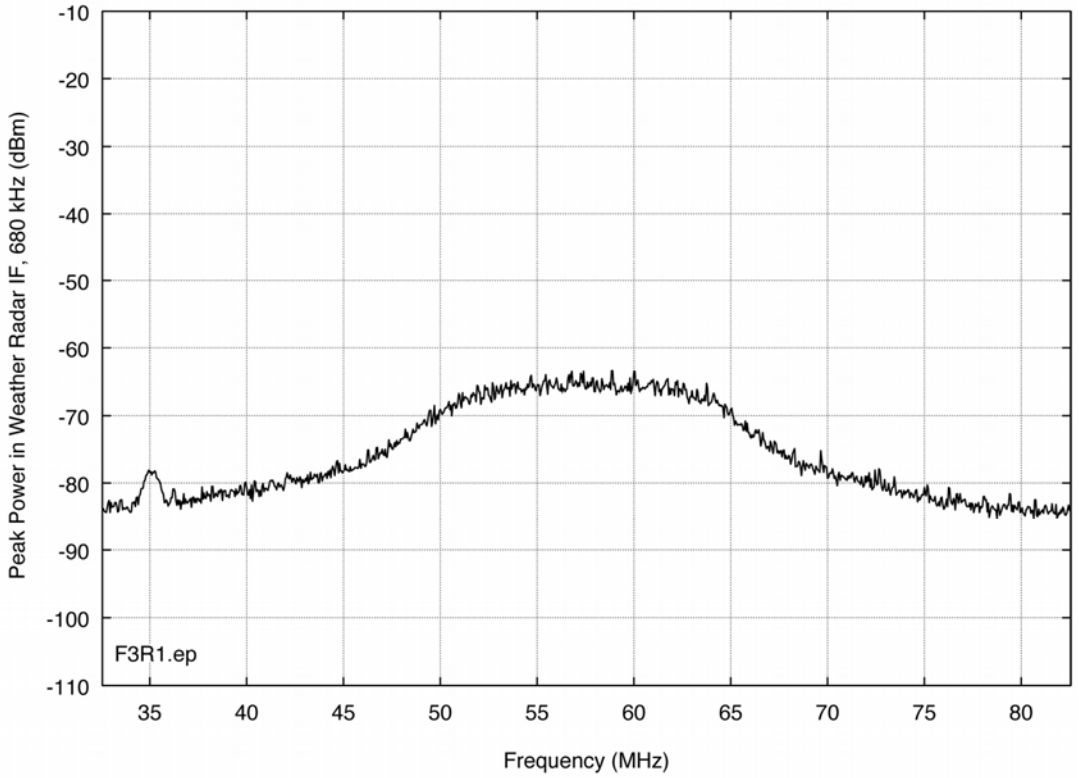

Figure 24. Weather radar IF spectrum when no interference was present (i.e., the airport radar transmitter was turned off). The elevated noise level that is observed is due to the normal output of the weather radar IF amplification stage. The elevated region of interest is between approximately 45-70 MHz. IF noise level is peak-detected, and has not been corrected for receiver gain. This (uncorrected) IF noise level shown in this figure is only supposed to be used as a reference for subsequent depictions of the weather radar IF spectrum in this report. The origin of the bump at 35 MHz was not investigated; it may be an image frequency.

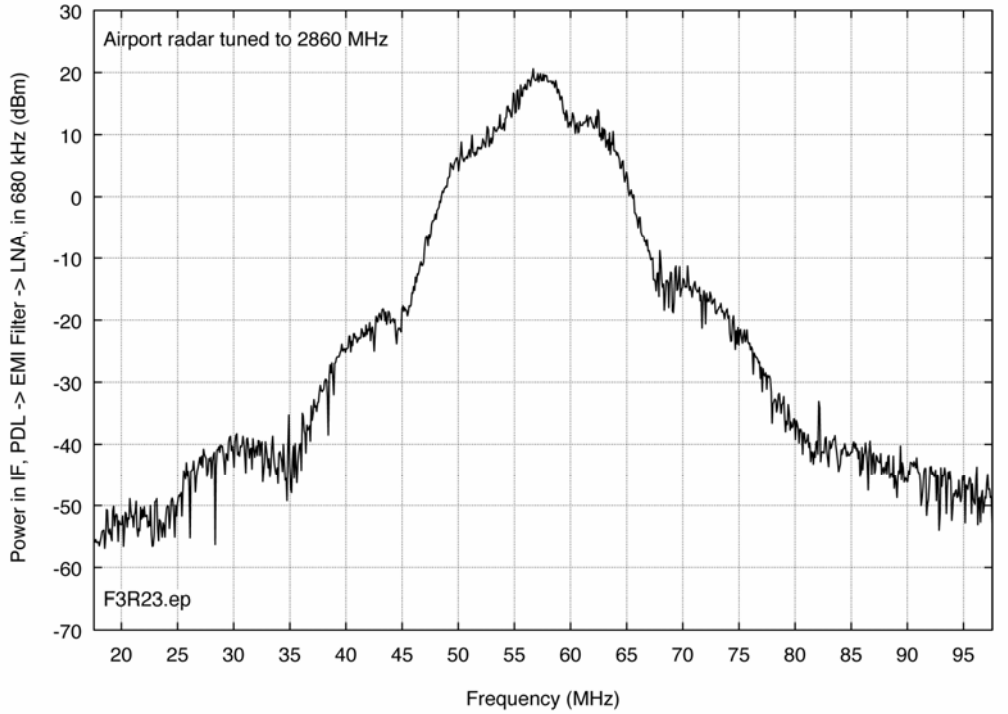

Figure 25. IF spectrum in the presence of interference from the airport radar, with the RF front-end arranged in its non-linear configuration.

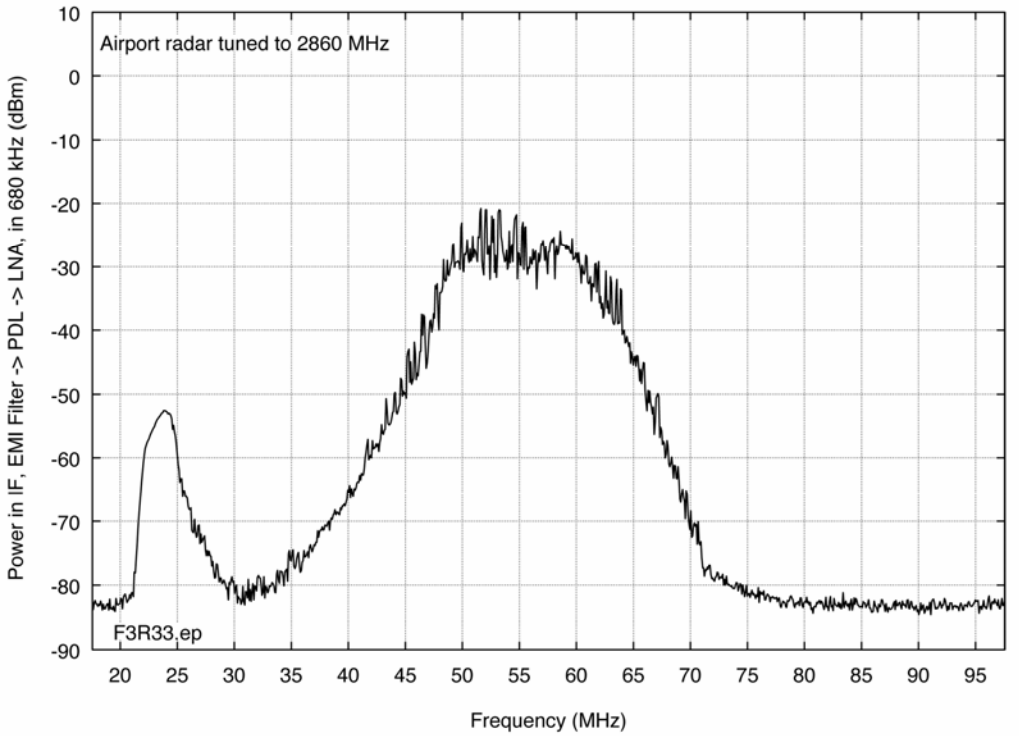

Figure 26. Weather radar IF spectrum in the presence of interference from the airport radar, when the PDL was placed *after* the EMI filter. The peak interference level has been reduced by 45 dB relative to the level in Figure 25. The origin of the bump at 24 MHz was not investigated.

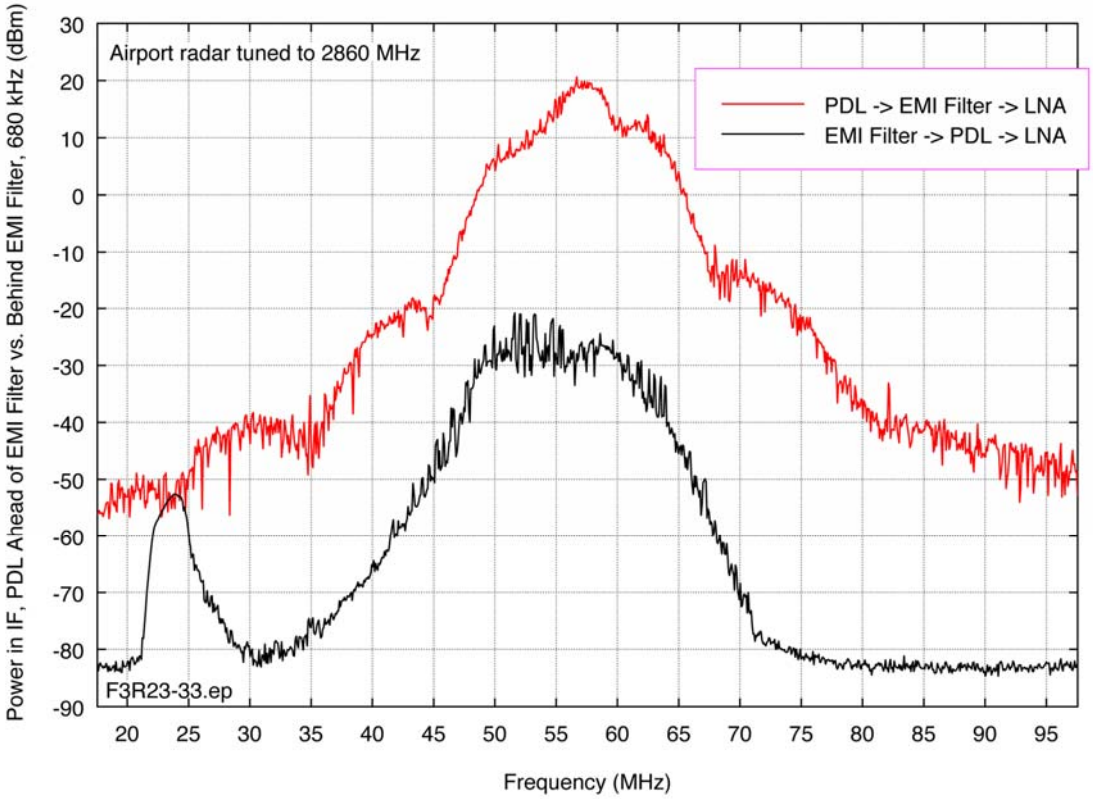

Figure 27. Comparison of curves from Figures 25 and 26.

3.4 Isolation of the Interference Mechanism

It had become clear that, with the non-linear problem discovered and solved, and lacking the presence of front-end overload gain compression in the RF front-end, the operative interference mechanism had probably been reduced to simple co-channel interference from the airport radar's unwanted emissions on the weather radar's frequency. This hypothesis was confirmed by measurement of the interference pulse time waveform envelope, as shown in Figure 28. Here, the 89-μs pulse displays the classic rabbit-ears diagnostic signature of an unwanted spectrum emission observed in the time domain. The waveform of Figure 28 was recorded when the PDL had been placed after the EMI filter.

Since this was the case, the (approximately) 40-dB *I/N* level that was achieved with this front-end configuration would now behave linearly, which is to say that every decibel of attenuation that could be achieved in the external interference input would translate into a corresponding reduction in the *I/N* level inside the receiver. This behavior is demonstrated in the comparative data curves of Figure 29. In this figure, the response of the weather radar IF stage is observed when the unwanted emissions of the airport were reduced under two cases: 1) the PDL located in front of the EMI filter and 2) the PDL located after the EMI filter. In the first case, attenuating the airport radar unwanted emissions (with a notch filter on the airport radar's output) caused no effect on the *I/N*

level, as evidenced by the identical blue and red curves in the figure. In the second case, attenuation of the airport radar signal *did* result in a reduction in the *I/N* level, as evidenced by the difference between the black and green curves in the figure.

When a notch filter was installed in the airport radar output (with the weather radar RF front-end in its modified configuration), the level of the interference strobe was reduced. This is the configuration of the airport radar and the weather radar that is represented by the green data curve in Figure 29.

Above all else, the data in Figure 29 demonstrate that the interference problem cannot be solved unless the weather radar RF front-end is reconfigured, and furthermore that after such a reconfiguration, the problem becomes one of merely filtering the unwanted emissions of the airport radar to a sufficient degree to eliminate interference effects in the weather radar.

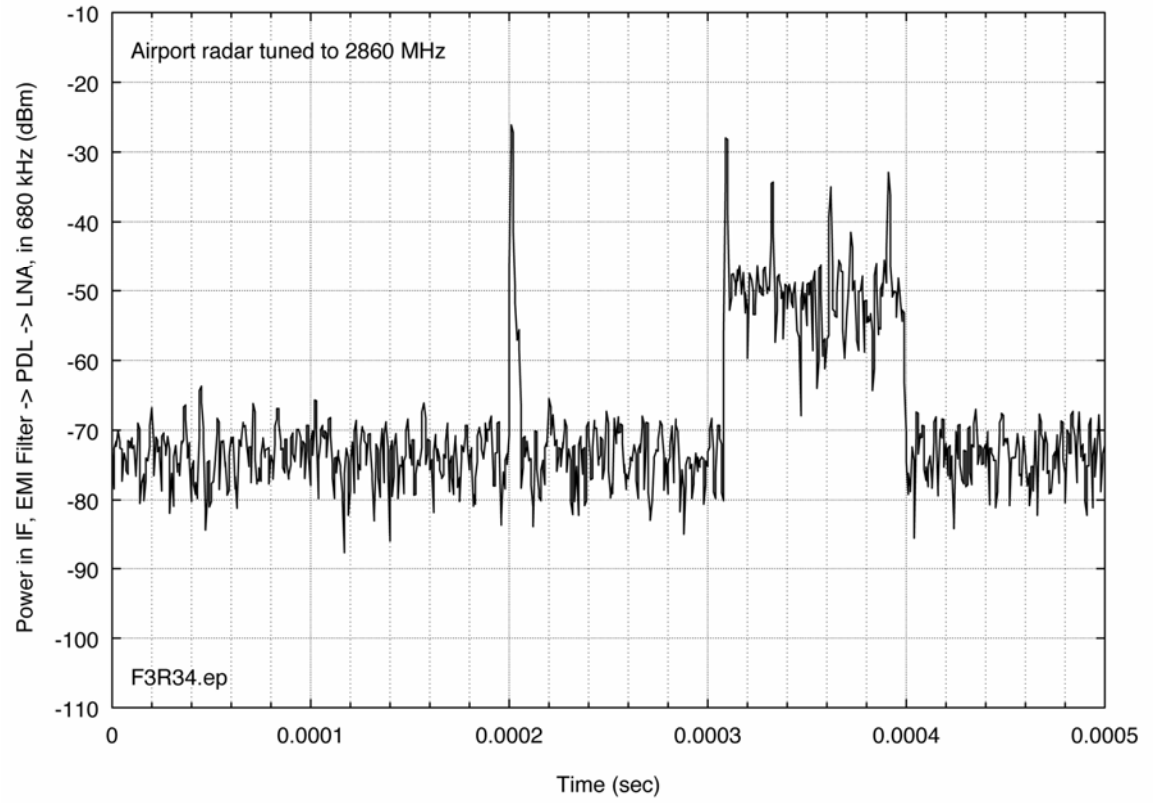

Figure 28. Diagnostic confirmation of co-channel interference due to unwanted emissions. These data were collected when the PDL had been placed after the EMI filter.

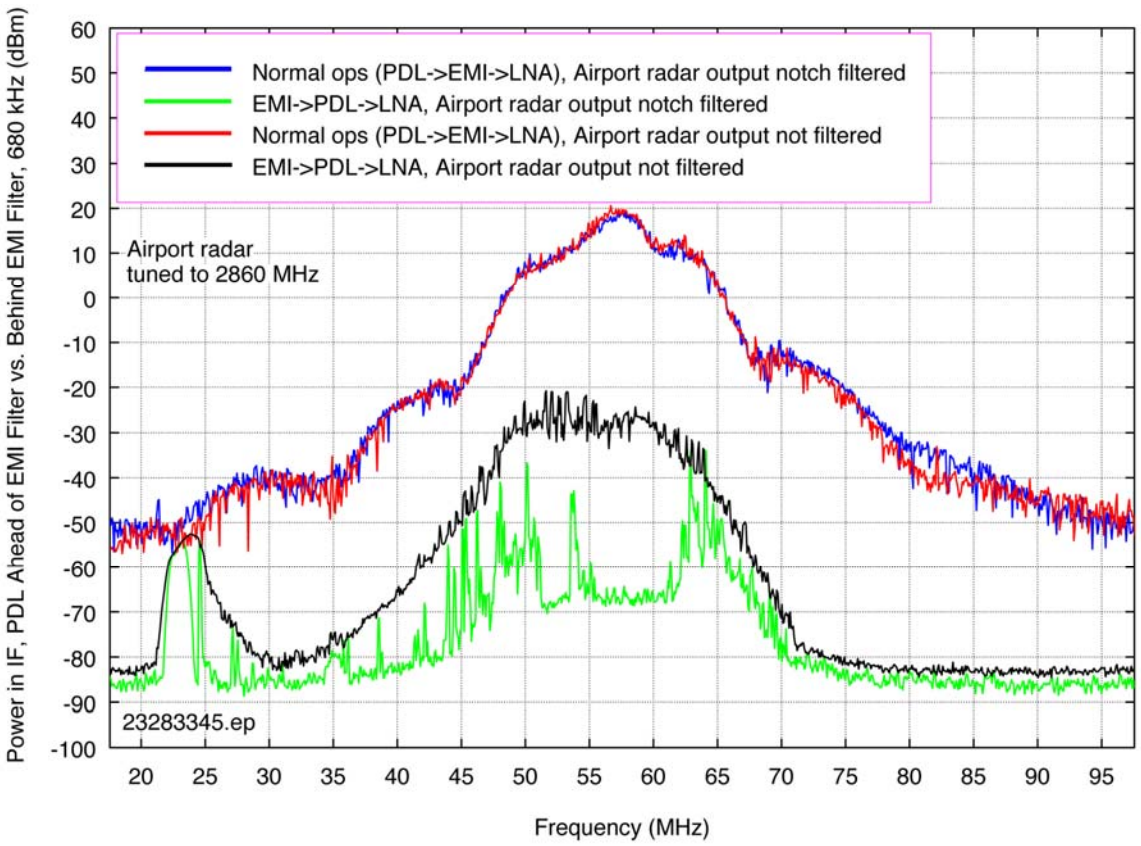

Figure 29. Comparative weather radar responses to reductions in unwanted emission interference energy, as a function of weather radar configuration.

3.5 Experiments with Notch Filtering of the Airport Radar

Considering that reductions in the unwanted emission levels of the airport radar would reduce the *I/N* level of the interference in the weather radar IF stage, an experiment was performed in which the airport radar was tuned from its initial frequency of 2860 MHz to a new frequency 85 MHz lower, at 2775 MHz. Such off-tuning was found to provide a 10-dB reduction in the unwanted emission level on the weather radar frequency. When the notch filter was installed on the airport radar output, an improvement was noted in the *I/N* level in the weather radar's IF stage, as shown in Figure 30.

In Figure 30, the noise floor that is seen in the center of the notch shape is in fact the noise floor of the weather radar IF stage[5]; this is a desirable result. The notch is simply not quite wide enough to fully reduce the interference energy across the full bandwidth of the IF stage.

[5] The IF noise level shown in Figure 30 is peak-detected and uncorrected for receiver gain, as previously noted in Figure 24. The weather radar's true (corrected, average) IF noise floor level is actually -80 dBm; the IF noise floor level shown in Figure 24 should be used as a reference for Figure 30.

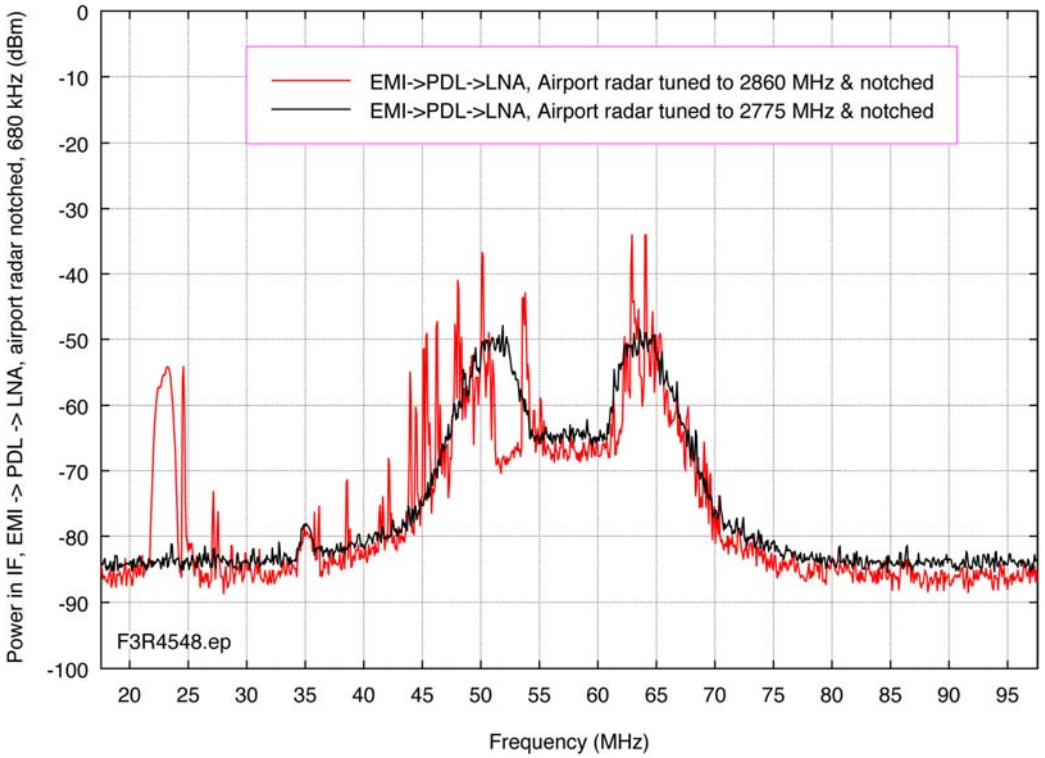

Figure 30. Comparison of the effect of the notch filter on the airport radar output when the tuned frequencies were 2860 MHz vs. 2775 MHz.

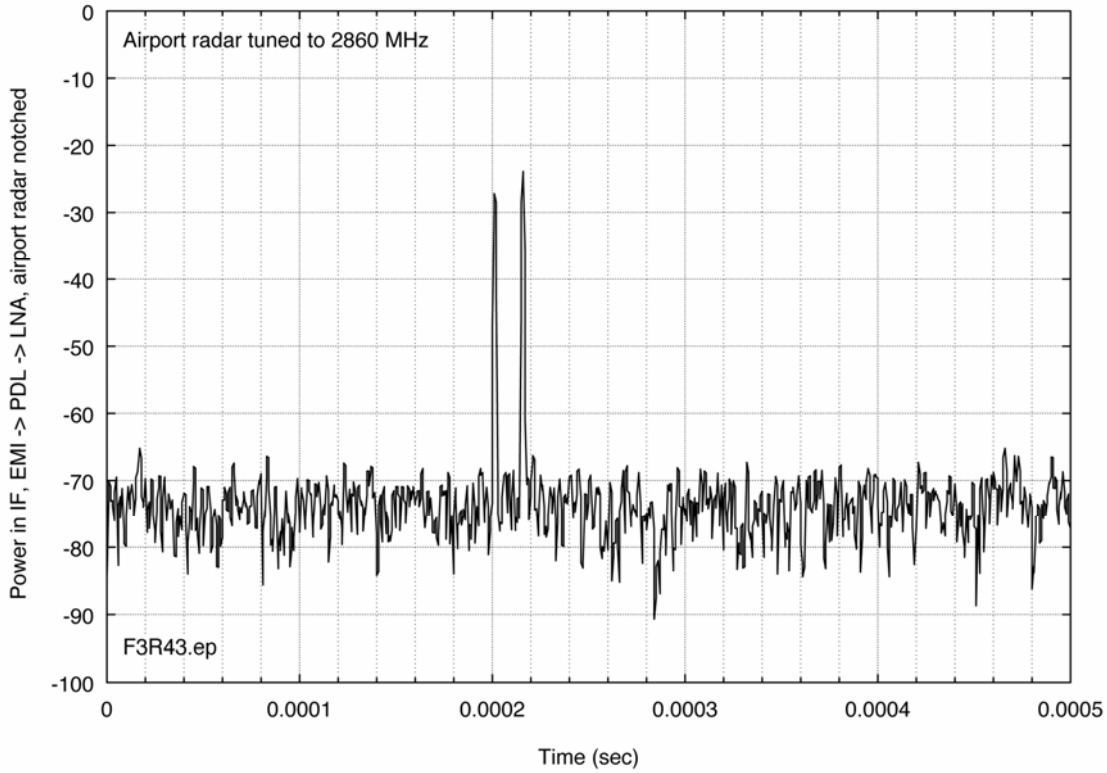

Figure 31. Time domain envelope of interference pulses when notch filtering (as shown in Figure 30) was installed on the airport radar output.

The effect of the notch filter was very pronounced in the time domain as well. There, the effect was to shorten the pulse pairs, from the original 1-μs+89-μs to a new set that looks more like 1-μs+1-μs. This is seen in Figure 31. The data in this figure show that, with the notch installed, the effective duty cycle of the interference in the weather radar receiver has been reduced from a nominal value of 8% (the duty cycle of the true airport radar pulse repetition sequence) to a new value that is about 0.2%.

3.6 Experiments with Variation of *I/N* Level in the Weather Radar Receiver

The final stage of the field work was to ascertain the critical *I/N* level at which interference from the notch-filtered airport radar would be reduced to a level at which no adverse effects were noted in the weather radar performance. Such experiments are difficult to perform because the weather radar is a data collection system that feeds its outputs into an off-site data processing system. That system generates weather 'products' that represent successively more complex layers of data processing. It is impossible to obtain immediate feedback on the results of testing with varying *I/N* levels; field teams who perform such work are therefore forced to work largely blind.

With that said, preliminary experiments were performed in which attenuation was inserted into the weather radar receiver, and also in which individual power output modules in the airport radar were taken out of service, thereby gradually reducing that radar's output power level. At the time of this report's completion, the results of those experiments indicate that more such experimental work will need to be performed at the weather radar site to ascertain definitive results on that topic. Among other concerns, data sets need to be collected under a wide range of weather conditions, whereas only a single day, with clear weather, was available at the field site for the first round of *I/N* tests that were performed.

4 SUMMARY

Although RF interference problems are often difficult and expensive to solve, a methodical approach, combined with a thorough understanding of the possible mechanisms of such interference, can (and almost inevitably will) yield positive results. As demonstrated by the results of this case study, even the occurrence of unexpected interference mechanisms should be revealed by a well-considered approach.

In this case, the interference was caused by unwanted emissions of an ASR on the operating frequency of a weather radar. But due to an unexpected, non-linear behavior in the RF front-end of the victim receiver, no workable solution could be implemented until the configuration of the victim receiver's RF front-end had been modified. Specifically, the PDL in that front-end had to be placed after the EMI bandpass filter before any technically workable solution could be implemented.

With the RF front-end configuration of the weather radar having been modified in this way, the interference problem was reduced to a straightforward exercise of determining the amount of attenuation that will be required in the levels of the unwanted emissions that cause interference. It is anticipated that such attenuation will be implemented by installing filtering on the output of the ASR that is causing interference at the location in question. This is the conventional solution to co-channel interference problems.

The determination of the necessary amount of attenuation that the output filter must achieve will await the completion of additional, definitive measurements by the NWS with the cooperation of the FAA. If a notch filter (as opposed to either a highpass or lowpass filter) is ultimately used on the ASR output, it will need to be about twice as wide as the one used for the experimental testing.

5 REFERENCES

[1] F.H. Sanders, R.L. Hinkle, and B.J. Ramsey, "Analysis of electromagnetic compatibility between radar stations and 4 GHz fixed-satellite Earth stations," NTIA Report 94-313, Jul. 1994.

[2] *Manual of Regulations and Procedures for Federal Radio Frequency Management*, May 2003, Revisions January 2006, NTIA Office of Spectrum Management, U.S. Government Printing Office, Stock No. 903-008-00000-8.

[3] F.H. Sanders, R.L. Hinkle, and B.J. Ramsey, "Measurement procedures for the Radar Spectrum Engineering Criteria (RSEC)," NTIA Report TR-05-420, Mar. 2005.

FORM **NTIA-29** (4-80)

U.S. DEPARTMENT OF COMMERCE
NAT'L. TELECOMMUNICATIONS AND INFORMATION ADMINISTRATION

BIBLIOGRAPHIC DATA SHEET

1. PUBLICATION NO.	2. Government Accession No.	3. Recipient's Accession No.
TM-06-439		

4. TITLE AND SUBTITLE	5. Publication Date
Resolving Interference from an Airport Surveillance Radar to a Weather Radar	April 2006
	6. Performing Organization Code NTIA/ITS
7. AUTHOR(S) Frank H. Sanders, J. Randy Hoffman, and Yeh Lo	9. Project/Task/Work Unit No. 611 6611000-300
8. PERFORMING ORGANIZATION NAME AND ADDRESS NTIA/ITS.T U.S. Department of Commerce 325 Broadway Boulder, CO 80305	10. Contract/Grant No.
11. Sponsoring Organization Name and Address	12. Type of Report and Period Covered

14. SUPPLEMENTARY NOTES

15. ABSTRACT (A 200-word or less factual summary of most significant information. If document includes a significant bibliography or literature survey, mention it here.)

In response to interference from an S-band (2700-2900 MHz) airport surveillance radar (ASR) to a meteorological (weather) radar in the same band, measurements were performed at the field location of the two radars to determine the interference mechanism and any possible mitigation options. Measurements included emission spectra of the ASR and observations of the interference energy in the RF front-end and IF stages of the weather radar. Measurement results showed that interference energy originated in the unwanted emissions of the ASR (i.e., front-end overload was not occurring in the weather radar). But the problem was exacerbated by the placement of a passive diode limiter ahead of a bandpass filter in the weather radar receiver's RF front-end. The interference could not be mitigated unless the front-end configuration of the weather radar was modified. With the necessary modification completed, the interference was successfully mitigated by installing a conventional notch filter on the ASR's output stage, the notch being tuned to the weather radar frequency. It is recommended that the front-end configuration of all weather radars of the type in question should be immediately changed in the same way as the weather radar in this study, and that appropriate output filters should be installed in ASRs that are located in close proximity to these weather radars to mitigate interference effects at all sites in the U.S.

16. Key Words (Alphabetical order, separated by semicolons)
airport surveillance radar interference; radar co-channel interference; radar emission spectrum measurements; radar interference mechanisms; radar interference mitigation; Radar Spectrum Engineering Criteria (RSEC); RF front-end overload; weather radar interference

17. AVAILABILITY STATEMENT	18. Security Class. (This report)	20. Number of pages
UNLIMITED.		31
	19. Security Class. (This page)	21. Price:

NTIA FORMAL PUBLICATION SERIES

NTIA MONOGRAPH (MG)

A scholarly, professionally oriented publication dealing with state-of-the-art research or an authoritative treatment of a broad area. Expected to have long-lasting value.

NTIA SPECIAL PUBLICATION (SP)

Conference proceedings, bibliographies, selected speeches, course and instructional materials, directories, and major studies mandated by Congress.

NTIA REPORT (TR)

Important contributions to existing knowledge of less breadth than a monograph, such as results of completed projects and major activities. Subsets of this series include:

NTIA RESTRICTED REPORT (RR)

Contributions that are limited in distribution because of national security classification or Departmental constraints.

NTIA CONTRACTOR REPORT (CR)

Information generated under an NTIA contract or grant, written by the contractor, and considered an important contribution to existing knowledge.

JOINT NTIA/OTHER-AGENCY REPORT (JR)

This report receives both local NTIA and other agency review. Both agencies' logos and report series numbering appear on the cover.

NTIA SOFTWARE & DATA PRODUCTS (SD)

Software such as programs, test data, and sound/video files. This series can be used to transfer technology to U.S. industry.

NTIA HANDBOOK (HB)

Information pertaining to technical procedures, reference and data guides, and formal user's manuals that are expected to be pertinent for a long time.

NTIA TECHNICAL MEMORANDUM (TM)

Technical information typically of less breadth than an NTIA Report. The series includes data, preliminary project results, and information for a specific, limited audience.

For information about NTIA publications, contact the NTIA/ITS Technical Publications Office at 325 Broadway, Boulder, CO, 80305 Tel. (303) 497-3572 or e-mail info@its.bldrdoc.gov.